Research Paper

THEMED ISSUE: Subduction Top to Bottom 2

GEOSPHERE

GEOSPHERE, v. 15, no. 3

https://doi.org/10.1130/GES02057.1

10 figures; 1 table; 1 set of supplemental files

CORRESPONDENCE: jdbarnes@jsg.utexas.edu

CITATION: Barnes, J.D., Cullen, J., Barker, S., Agostini, S., Penniston-Dorland, S., Lassiter, J.C., Klügel, A., and Wallace, L., 2019, The role of the upper plate in controlling fluid-mobile element (Cl, Li, B) cycling through subduction zones: Hikurangi forearc, New Zealand: Geosphere, v. 15, no. 3, p. 642–658, https://doi.org/10.1130/GES02057.1.

Science Editor: Shanaka de Silva
Guest Associate Editor: Robert J. Stern

Received 30 August 2018
Revision received 20 December 2018
Accepted 13 February 2019

Published online 9 April 2019

The role of the upper plate in controlling fluid-mobile element (Cl, Li, B) cycling through subduction zones: Hikurangi forearc, New Zealand

Jaime D. Barnes[1], Jeffrey Cullen[1], Shaun Barker[2,*], Samuele Agostini[3], Sarah Penniston-Dorland[4], John C. Lassiter[1], Andreas Klügel[5], and Laura Wallace[6,7]

[1]Department of Geological Sciences, University of Texas, Austin, Texas 78712, USA
[2]School of Science, University of Waikato, Hamilton 3240, New Zealand
[3]Istituto di Geoscienze e Georisorse, Consiglio Nazionale delle Ricerche, Area della Ricerca di Pisa, PI, 56124, Italy
[4]Department of Geology, University of Maryland, College Park, Maryland 20742, USA
[5]FB-Geowissenschaften, University of Bremen, Bremen 28359, Germany
[6]GNS Science, Lower Hutt 5011, New Zealand
[7]Institute for Geophysics, University of Texas at Austin, Austin, Texas 78758, USA

ABSTRACT

In order to trace the cycling of fluid-mobile elements (FMEs) through subduction zone forearcs, we collected water samples from two warm and 16 cold springs along the subaerially exposed forearc of the Hikurangi subduction zone in New Zealand. Water samples were analyzed for their cation and anion concentrations, as well as their B, Li, Cl, and O stable isotope compositions. Fluids discharging through the prism have high concentrations of Cl (2400–16,000 mg/L), Br (6–70 mg/L), I (0.4–72 mg/L), Sr (0.1–200 mg/L), B (3–130 mg/L), Li (0.1–13 mg/L), and Na (33–6600 mg/L), consistent with data from previous studies. Most of these elements decrease overall in concentration from north to south, have a concentration peak in the central part of the margin, and have had limited concentration variability during the last three decades. Because Li, Cl, and B are all fluid-mobile elements, their incompatibility potentially limits modification by fluid-rock interaction, making them reliable tracers of fluid source. δ^{37}Cl, δ^{11}B, and δ^{7}Li values range from −1.3‰ to +0.4‰ (n = 36), +11.8‰ to +41.9‰ (n = 25), and −3.1‰ to +29.0‰ (n = 29), respectively. Despite the change in concentrations along the margin, there is no corresponding trend in isotopic composition. Chlorine and boron isotope compositions are consistent with fluids dominated by seawater (δ^{37}Cl = 0‰; δ^{11}B = 40‰) and sedimentary pore fluids (δ^{37}Cl ≈ −8‰ to 0‰; δ^{11}B > ~17‰). Br/Cl (0.0025–0.005) and I/Cl (0.00005–0.007) weight ratios also support a dominant seawater and pore-fluid source. Lithium isotope data also suggest fluids sourced from seawater (δ^{7}Li = +31‰) as well as dehydrating sediments and/or modified by interaction with local sediment. The fluid geochemical data cannot be explained by a change in the fluid source along the margin, but rather by a change in the upper-plate structural permeability. In the north, extension likely results in a highly permeable forearc, whereas transpression in the south traps fluids within the upper plate and dilutes saline fluids with groundwater. Such changes in upper-plate structural permeability may influence fluid pressure conditions within the forearc, which in turn may influence the observed change in slip behavior on the interface from north Hikurangi (aseismic creep) to south Hikurangi (deep locking). This work highlights the role the upper plate may play in the geochemical modification and transport of slab-derived fluids, and supports the long-standing but poorly documented assumption that seawater and pore fluids are expelled at shallow levels in the subduction zone (<15 km) and therefore play a limited role in the transport of FMEs to great depths in subduction zones.

INTRODUCTION

Lithium, chlorine, and boron are all highly fluid-mobile elements (FMEs). Their incompatibility in rocks limits modification by fluid-rock interaction, thereby making them potentially excellent tracers of fluid source. Isotopic systems of all three elements have been used as a fluid tracer in subduction zones or to trace recycled crustal material in the upper mantle (e.g., Barnes et al., 2008, 2009; Chiaradia et al., 2014; Elliott et al., 2006; Ishikawa and Nakamura, 1994; John et al., 2010; Leeman et al., 2004, 2017; Moriguti and Nakamura, 1998; Peacock and Hervig, 1999; Penniston-Dorland et al., 2010; Straub and Layne, 2002; Zack et al., 2003). Much work has focused on defining the elemental concentration and isotopic composition of subduction zone inputs (e.g., sediments, altered oceanic crust, serpentinites) and outputs from the volcanic front (e.g., volcanic gases, melt inclusions in phenocrysts). However, poor constraints on the elemental concentrations and isotopic compositions from forearc outputs limit flux calculations. Most subduction-zone flux calculations of FMEs ignore contributions from the forearc because forearc output fluxes and the subducted sources contributing to the forearc outputs are poorly constrained

*Now at ARC Centre of Excellence in Ore Deposits (CODES), School of Natural Sciences, University of Tasmania, Hobart, Tasmania 7001, Australia

(e.g., Barnes et al., 2018; Freundt et al., 2014; Füri et al., 2010; Völker et al., 2014). The subaerial Hikurangi forearc of New Zealand overlies portions of the plate interface as shallow as 12 km and hosts numerous forearc seeps and springs (Fig. 1), typically submerged at most subduction zones. Easy access to forearc springs along the margin allows for quantification of volatile flux and source through the shallow portion of the subduction system.

In addition, there are along-str ke variations in subduction parameters along the length of the Hikurangi margin (Fig. 1). The northern portion of the margin is marked by a thin layer of sediments (~1 km) and many seamounts on the incoming plate, a steep taper angle (7° to 10°) for the accretionary wedge, and shallow (<15 km) aseismic creep. In contrast, the southern portion has a thick (3–6 km) package of sediments on the incoming plate, has a low taper angle (4° to 6°) for the accretionary wedge, and is interseismically coupled to ~30 km depth (e.g., Wallace and Beavan, 2010; Wallace et al., 2009). Previous studies have noted a change in the forearc fluid chemistries, specifically an overall decrease in the Cl, B, Br, Na, and Sr concentrations in spring waters, from the north to the south (Giggenbach et al., 1995; Reyes et al., 2010). These observations raise numerous questions, such as: Is there a slab-derived fluid component to the springs? Is there a change in the slab-derived fluid source along the margin? Is there a link between slab-derived fluids and the change in subduction-interface slip behavior? In order to address these questions, we sampled fluids from 16 cold and two thermal springs (Morere and Te Puia) from the Hikurangi margin and analyzed them for their Cl, Li, and B isotope compositions. These data, in conjunction with trace element geochemistry (e.g., Br/Cl, I/Cl, B/Cl, Br/B, and Li/B weight ratios), are used to determine whether fluid sources vary along the length of the margin, and particularly whether any variation reflects that of metamorphic reactions or diagenetic processes that may be linked to shallow aseismic slip events and/or the onset of interseismic coupling.

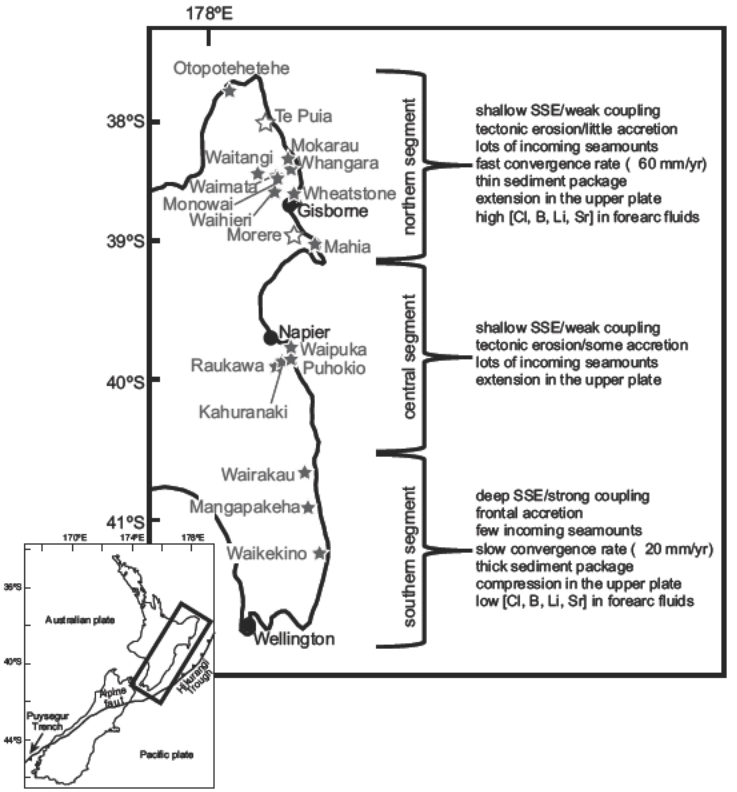

Figure 1. Map of the Hikurangi margin of the North Island of New Zealand showing the location of sampled cold springs (solid gray stars) and thermal springs (open gray stars). Along-strike variations in subduction parameters and margin properties are summarized (modified from Wallace et al., 2010). SSE—slow-slip events. Inset map shows the tectonic setting of New Zealand.

HIKURANGI MARGIN

Geologic Setting

The oblique convergence of the Australian and Pacific plates has resulted in doubly convergent subduction zones along the New Zealand plate boundary: (1) the Hikurangi Trench that accommodates westward subduction of the Pacific plate offshore the east coast of the North Island (e.g., Cashman et al., 1992; Rait et al., 1991), and (2) the Puysegur Trench that accommodates eastward subduction of the Australian plate offshore the southwestern South Island (Eberhart-Phillips and Reyners, 2001) (Fig. 1). The two subduction zones are linked by the Marlborough fault system and Alpine fault (e.g., Lebrun et al., 2000). Active volcanism began in the Holocene due to the subduction of the Pacific plate and is primarily confined to the Taupo Volcanic Zone in the central part of the North Island (e.g., Wilson et al., 1995).

The Hikurangi Plateau, a basaltic, Cretaceous oceanic plateau, is being subducted at the Hikurangi Trench (Mortimer and Parkinson, 1996). The Hikurangi Plateau thickens from ~10 km in the north to ~15 km near Chatham Rise in the south (Davy and Wood, 1994). The plateau is dotted with seamounts, which emerge above the sedimentary cover sequences in the north (e.g., Wood and Davy, 1994). The plateau is covered with Cretaceous and Cenozoic sediments: >500 m of Cretaceous (>100 Ma) volcanoclastic sediments and/or limestones and cherts, ~600 m of Cretaceous (100–70 Ma) clastic sedimentary rocks, and ~200 m of the Cretaceous–Oligocene (70–32 Ma) chalks and mudstones, capped by a sequence of Cenozoic sediments consisting of chalk interbedded with tephras and clays and late Cenozoic turbidites (Barnes et al., 2010; Davy et al., 2008). The turbidite sequence thickens from ~1 km thick in the north to ~5 km thick in the south (Lewis et al., 1998), coincident with a three-fold decrease in subduction rate from ~60 mm/yr in the north to ~20 mm/yr in the south (Wallace et al., 2004). The thin sediment sequence, high convergence rate, and

rough topography of the incoming plate promotes frontal tectonic erosion and development of a narrow active wedge in the north, whereas a classic, wide accretionary wedge has built out rapidly in the south (e.g., Barnes et al., 2010; Lewis et al., 1998).

The Hikurangi forearc is ~150–200 km wide and consists of an inner foundation of Late Cretaceous and Paleogene pre-subduction rocks, an outer wedge of late Cenozoic accreted turbidites, and a cover sequence of Miocene to recent shelf and slope sediments, built on a Mesozoic basement of greywackes (Barnes et al., 2010). Estimated volumes of fluid discharge range from ~20 to ~40 m^3 per meter length per year through the shallow portion (<20 km) of the Hikurangi margin (Ellis et al., 2015; Pecher et al., 2010; Townend, 1997). This enormous volume of fluid release is manifested in the >250 onshore and >12 offshore spring systems along the eastern margin of the North Island, mud volcanoes, vent fauna associated with offshore seeps, bottom simulating reflections interpreted as the base of the gas hydrate stability zone, seismic reflection data interpreted as subducting fluid-rich sediments, and elevated pore pressures in exploration wells (e.g., Barnes et al., 2010; Darby and Funnell, 2001; Lewis and Marshall, 1996; Pecher et al., 2010; Pettinga, 2003; Reyes et al., 2010).

Prior Work on Volatile Flux through the Hikurangi Margin

There have been a few previous studies on the geochemistry of onshore springs in the Hikurangi forearc. The spring waters discharging from the forearc are enriched in ^{18}O and D ($\delta^{18}O$ = –4.6‰ to +7.1‰; δD = –28‰ to –2‰) with respect to local groundwater ($\delta^{18}O \approx -5‰$; $\delta D \approx -30‰$) (Giggenbach et al., 1995; Reyes et al., 2010). Giggenbach et al. (1995) interpreted the $\delta^{18}O$ and δD values of the forearc springs as mixing of local groundwater with 20%–55% water derived from marine clay dehydration. Reyes et al. (2010) stated that the oxygen and hydrogen isotope compositions of the forearc fluids are also consistent with marine sedimentary pore fluids with a fluid component derived from clay dehydration. Either of these interpretations assumes little to no isotopic exchange with the local rock, which would increase the stable isotope values. Previous work has shown an overall decrease in the Cl, B, Br, Na, and Sr concentrations in spring waters from the north to the south in the Hikurangi forearc, with Cl, I, and Br having distinct highs in the central part of the margin (Giggenbach et al., 1995; Reyes et al., 2010). The center of the margin also has high $^3He/^4He$ ratios in gases (R/R_A values up to 3.35 at Morere, where R/R_A is the $^3He/^4He$ ratio with respect to air), suggesting up to ~40% mantle He contribution (Giggenbach et al., 1993, 1995). The central margin with high R/R_A values, corresponding with high Cl, I, and Br concentrations, has been interpreted as a section of the prism with a greater pathway to the mantle wedge and subducted component (Giggenbach et al., 1995). However, $^{129}I/I$ ratios suggest an old iodine source to the forearc fluids, sourced from the previously accreted material within the forearc and not derived from actively subducting sediments (Fehn and Snyder, 2003; Fehn et al., 2007).

METHODS

Sampling

Water samples were collected from 18 different spring systems (Fig. 1; Table 1). Two of these spring systems are thermal spring systems (Morere and Te Puia) with discharge temperatures of ~45 and ~65 °C, respectively (Table 1). The remaining 16 systems are cold springs (discharge temperatures similar to or below the ambient air temperature). Spring systems previously studied (Fehn et al., 2007; Giggenbach et al., 1995; Reyes et al., 2010) were sampled whenever possible to track geochemical changes through time. Several previously undocumented spring systems were also sampled. Multiple discharge sites in a given spring system were sampled where possible (Table 1); however, many of the discharge sites are transient or do not flow year-round.

Water samples were collected using Tygon tubing lowered into the pool and attached to a peristaltic pump. Samples were collected in separate polyethylene Nalgene vessels for anion, cation, and alkalinity analyses and stable isotope analyses. Samples to be used for cation analysis were acidified in the field to a pH of ~2 using 18N HNO_3 to avoid precipitates from forming. All water samples were filtered through a 0.35 µm membrane when possible; the presence of mud prevented the filtering of some samples.

Cation and Anion Analyses

Cation concentrations (Li, B, Na, Sr, K, Ca, Mg, Al, Si, P, Ti, V, Mn, Fe, Co, Ni, Cu, Zn, Rb, Zr, Mo, Cs, Ba, U) were measured on an Agilent 7500ce Quadrupole inductively coupled plasma–mass spectrometer (ICP-MS) at University of Texas at Austin (UT-Austin, USA). Multiple dilutions of U.S. National Institute of Standards and Technology (NIST) 1643e were used as the primary reference standard. Analytical errors are between 1% and 3%. Chlorine concentrations were measured on a Dionex ICS 2000 ion chromatograph at UT-Austin. Reference standards were within 5% of the calibration with a minimum detection limit of 0.05 µg/g for Cl. Fluorine was below the minimum detection limits of 0.1 µg/g.

Concentrations of Br and I were measured by ICP-MS using a Thermo Element 2 at the University of Bremen (Germany) equipped with a self-aspiring micro-flow nebulizer and a quartz cyclonic–Scott dual spray chamber. In order to reduce matrix load and minimize memory effects, samples were diluted 1000 fold with a 5% NH_4OH solution (suprapure quality), and a blank was analyzed before each sample (cf. Bu et al., 2003). The system was calibrated with seven pure standard solutions having concentrations of 0.2–20 ng/ml Br and I. Sample and calibration solutions were spiked with 1 mg/l Te as an internal standard. The isotopes ^{79}Br and ^{127}I were analyzed in medium resolution and ^{79}Br additionally in high resolution to remove interference by $^{40}Ar^{38}Ar^1H$. Both ^{79}Br determinations yielded similar results, with a coefficient of determination of $r^2 = 0.9993$ for the entire data set. The high-resolution data are lower by <3% on average, and only these values are reported here. The calculated detection

TABLE 1. LOCATION, SAMPLING TEMPERATURE, pH, CONDUCTIVITY, AND MAJOR GEOCHEMICAL DATA FOR COLD AND THERMAL SPRING FLUIDS ALONG THE HIKURANGI MARGIN, NEW ZEALAND

Sample	IGSN	Latitude	Longitude	Date sampled	pH	T (°C)	Conductivity (mS/cm)	$\delta^{11}B$ (‰)	$\delta^{11}B$ (error) (‰)	$\delta^{11}B$ (wt avg) (‰)	$\delta^{11}B$ (wt avg error) (‰)	$\delta^{37}Cl$ (‰)	$\delta^{7}Li$ (‰)	$\delta^{7}Li$ lab	$\delta^{18}O$ (‰)	Cl	I	Br	Li	B	Na	Sr	K	Ca	Mg
Otopotehetehe																									
Pool 1	IEJDB0017	37°36′55.2″S	178°08′25.0″E	21 June 2015	7.5	14.8	10.5	-	-	27.3	1.1	–1.2	4.2	UT	-	6143	3.80	18.4	9.5	100.0	3373	28.8	24	245	10.9
Main	IEJDB001C	37°36′55.2″S	178°08′25.0″E	21 June 2015	-	-	3.6	-	-	-	-	-	-	-	-	-	-	-	13.2	122.1	5157	40.0	57	670	28.7
2	IEJDB001B	37°37′19.8″S	178°08′38.0″E	21 June 2015	-	13.4	13.5	-	-	19.1	1.1	–0.1	3.5	UT	-	7919	0.40	24.5	5.0	85.9	4456	29.6	29	343	43.2
#1	IEJDB0001	37°36′55.2″S	178°08′25.0″E	2 March 2016	7.54	22	9.9	-	-	24.2	1.0	–0.4	4.1	C	6.5	7912	5.05	25.7	12.5	130.1	4515	38.5	36	297	14.1
							-	-	-	-	-	-	4.4	UT	-										
#2	IEJDB0002	37°36′55.2″S	178°08′25.0″E	2 March 2016	7.42	20	13.6	-	-	-	-	-	-	-	-	-	-	-	11.6	131.7	4490	39.9	37	328	16.7
Te Puia																									
TP1	IEJDB001E	38°03′27.4″S	178°18′10.7″E	26 March 2014	-	-	-	-	-	-	-	–0.3	-	-	-	8716	-	-	3.2	72.4	4452	74.1	40	718	7.1
TP2	IEJDB001F	38°03′27.4″S	178°18′10.7″E	26 March 2014	-	-	-	-	-	-	-	–0.1	-	-	-	5204	-	-	1.7	43.7	2653	43.0	25	453	6.0
Pool 1	IEJDB0012	38°03′27.4″S	178°18′10.7″E	21 June 2015	6.83	65.6	43.4	-	-	19.8	0.6	–0.3	–3.1	UT	4.0	8959	18.0	29.2	3.2	72.6	4427	73.8	41	716	7.2
Pool 2	IEJDB0013	38°03′27.4″S	178°18′10.7″E	21 June 2015	6.47	66.4	40.4	-	-	-	-	-	-	-	-	-	-	-	3.1	72.4	4369	73.7	41	722	6.9
Hillside	IEJDB0003	38°03′28.6″S	178°18′14.0″E	3 March 2016	-	-	-	-	-	-	-	0.0	–2.6	C	-	6940	4.62	22.6	2.2	62.1	3510	58.4	32	594	7.9
Waitangi																									
Oil	IEJDB000Z	38°20′32.31″S	177°54′04.63″E	7 March 2016	-	-	-	-	-	-	-	-	-	-	-	-	-	-	bdl	bdl	40	0.2	6	16	3.8
Well	IEJDB000F	38°20′17.90″S	177°53′48.76″E	7 March 2016	-	-	-	-	-	-	-	–0.8	4.3	C	-	3222	17.8	10.9	1.7	13.6	2619	4.7	7	12	7.5
Mokarau	IEJDB000A	38°27′29.04″S	178°13′49.46″E	6 March 2016	7.55	22.2	21.8	-	-	23.2	0.5	–0.3	17.0	UT	5.0	8275	1.99	25.9	1.6	60.2	3981	45.2	22	631	50.7
Waimata																									
	IEJDB0015	38°29′17.3″S	178°03′12.4″E	20 June 2015	7.45	13.5	8.31	-	-	11.8	2.1	–0.6	1.5	UT	-	6649	0.75	19.5	1.9	58.3	3903	20.0	25	239	38.5
1	IEJDB0005	38°29′17.7″S	178°03′12.2″E	5 March 2016	7.55	19.6	12.6	-	-	25.3	0.5	–0.3	0.4	UT	3.8	6546	6.40	21.1	1.9	65.7	3871	23.2	23	178	29.7
2	IEJDB0006	38°29′17.7″S	178°03′12.2″E	5 March 2016	7.95	18.8	14.3	-	-	-	-	-	-	-	-	-	-	-	1.8	63.3	3887	21.9	25	160	31.0
Monowai																									
1	IEJDB0007	38°30′25.43″S	178°01′32.78″E	5 March 2016	7.77	23.6	13.6	36.9	0.5	36.7	0.4	–1.2	3.7	C	2.2	5723	12.0	17.2	1.1	25.2	3363	9.5	16	85	26.7
								36.2	0.8	-	-	–0.5	3.5	UT	-										
												–0.8													
Gas spring 1	IEJDB000G	38°29′45.25″S	178°01′8.89″E	8 March 2016	7.76	21.6	13.6	-	-	30.7	0.3	–0.2	3.0	UT	-	6738	5.26	20.4	1.3	57.7	3998	14.5	25	130	38.0
Gas spring 2	IEJDB000H	38°29′45.25″S	178°01′8.89″E	8 March 2016	7.95	24.5	16.55	-	-	-	-	0.0	-	-	-	5880	12.2	17.2	1.0	43.8	3414	12.3	23	133	38.6
Whangara																									
B5 1	IEJDB000B	38°31′21.15″S	178°13′24.31″E	7 March 2016	7.51	-	15.72	-	-	40.1	1.3	–0.9	2.2	UT	3.0	5572	19.7	26.0	1.4	26.5	3916	14.5	19	55	28.8
B5 2	IEJDB000C	38°31′21.15″S	178°13′24.31″E	7 March 2016	-	21.7	11.9	-	-	-	-	-	-	-	-	-	-	-	1.4	26.7	3925	16.9	18	77	34.0
Waihireri																									
1	IEJDB001D	38°34′19.7″S	177°56′26.4″E	20 June 2015	8.05	14.9	8.95	-	-	37.7	1.2	–1.0	6.7	UT	-	5163	1.03	15.5	0.9	30.2	3164	6.7	20	121	24.7
1	IEJDB0008	38°34′19.7″S	177°56′26.4″E	5 March 2016	8	25.8	14.77	-	-	37.5	0.5	–0.6	9.1	UT	1.8	5058	15.8	15.9	0.7	32.0	3051	6.3	15	98	19.8
								-	-	-	-	–0.5	-	-	-										
2	IEJDB0009	38°34′19.7″S	177°56′26.4″E	5 March 2016	7.86	28.1	13.25	-	-	-	-	-	-	-	-	-	-	-	0.9	30.2	3112	7.5	15	99	18.7
Wheatstone																									
	IEJDB0018	38°40′50.0″S	178°03′50.5″E	21 June 2015	7.63	14.6	11.25	-	-	24.9	0.3	–0.6	0.9	UT	5.7	6831	13.5	23.6	2.9	37.6	3704	42.9	31	334	58.0
								-	-	-	-	–0.3	-	-	-										
1	IEJDB000D	38°40′50.0″S	178°03′50.5″E	7 March 2016	7.4	25.3	16.5	-	-	-	-	–0.5	2.3	C	-	6701	34.5	23.4	2.8	39.8	3759	43.3	28	279	54.9
2	IEJDB000E	38°40′50.0″S	178°03′50.5″E	7 March 2016	7.46	24.1	13.77	-	-	-	-	-	-	-	-	-	-	-	2.8	39.7	3768	40.9	28	257	53.7

(continued)

TABLE 1. LOCATION, SAMPLING TEMPERATURE, pH, CONDUCTIVITY, AND MAJOR GEOCHEMICAL DATA FOR COLD AND THERMAL SPRING FLUIDS ALONG THE HIKURANGI MARGIN, NEW ZEALAND (*continued*)

Sample	IGSN	Latitude	Longitude	Date sampled	pH	T (°C)	Conductivity (mS/cm)	$\delta^{11}B$ (‰)	$\delta^{11}B$ (error) (‰)	$\delta^{11}B$ (wt avg) (‰)	$\delta^{11}B$ (wt avg error) (‰)	$\delta^{37}Cl$ (‰)	$\delta^{7}Li$ (‰)	$\delta^{7}Li$ lab	$\delta^{18}O$ (‰)	Cl	I	Br	Li	B	Na	Sr	K	Ca	Mg
Morere																									
MR1	IEJDB001G	38°59′11.2″S	177°47′28.9″E	26 March 2014	-	-	-	-	-	-	-	0.0	-	-	-	16409	-	-	5.2	45.0	6299	202.1	79	2681	78.4
								-	-	-	-	0.0	-	-	-										
Pool 1	IEJDB0011	38°59′05.4″S	177°47′54.2″E	22 June 2015	6.6	44.2	55.3	-	-	25.8	0.7	–0.2	7.8	UT	3.6	15989	24.7	63.5	5.0	42.8	6075	192.3	77	2589	72.7
Pool 2	IEJDB0014	38°59′05.4″S	177°47′54.2″E	22 June 2015	6.55	44.2	55.5	-	-	-	-	0.1	-	-	-	15847	25.1	63.1	4.9	43.7	6170	193.5	77	2559	74.3
Mahia																									
1	IEJDB000I	39°8′27.48″S	177°55′44.74″E	8 March 2016	6.85	22.6	38.8	22.7	0.4	23.1	0.2	–1.1	7.1	C	3.0	15904	2.64	62.7	3.4	46.6	6301	145.5	45	2483	52.8
								23.3	0.3	-	-	-	7.3	UT	-										
2	IEJDB000J	39°8′27.48″S	177°55′44.74″E	8 March 2016	-	-	34.1	-	-	-	-	-	-	-	-	-	-	-	3.3	46.6	6308	140.6	43	2427	54.1
3	IEJDB000K	39°8′29.41″S	177°55′43.59″E	8 March 2016	6.8	21.5	38.8	-	-	24.0	0.9	–0.4	6.8	UT	-	16429	8.03	66.5	3.4	45.8	6429	146.3	46	2488	65.7
New 1	IEJDB000L	39°7′58.38″S	177°55′57.40″E	8 March 2016	-	20.1	26	-	-	37.7	0.7	–0.7	–0.8	UT	1.6	11580	-	-	2.0	35.7	5198	61.3	30	1159	73.1
New 2	IEJDB000M	39°7′58.38″S	177°55′57.40″E	8 March 2016	-	22.2	32	-	-	-	-	–0.6	–2.3	C	-	14851	24.4	69.1	2.7	41.2	6386	89.3	44	1674	157.9
Raukawa																									
Cement	IEJDB000Q	39°42′58.43″S	176°37′54.33″E	9 March 2016	7.77	15.3	9.4	-	-	34.9	2.2	0.3	19.4	UT	–7.1	2998	1.37	16.0	0.4	3.7	1784	2.8	59	55	73.1
Pipe	IEJDB000R	39°43′38.71″S	176°38′12.11″E	9 March 2016	7.94	18	3.3	-	-	-	-	-	-	-	-	-	-	-	0.1	2.9	748	0.1	20	1	2.0
Waipuka	IEJDB0010	39°45′54.56″S	176°59′4.61″E	12 March 2016	8.24	17.1	31.1	42.0	1.1	41.9	0.9	–1.3	4.8	UT	5.0	9999	71.7	36.6	1.9	34.2	6614	9.9	57	183	66.3
								41.6	1.6	-	-	-	-	-	-										
Kahuranaki	IEJDB000P	39°46′50.06″S	176°50′13.51″E	10 March 2016	7.45	17.6	11.06	-	-	31.4	1.4	–0.2	–2.6	UT	–1.1	3572	3.55	10.4	0.4	51.4	1774	9.0	19	524	12.2
Puhokio																									
Puhokio 1	IEJDB000N	39°49′52.19″S	176°58′28.36″E	9 March 2016	7.82	21	8.2	-	-	41.9	0.9	–0.1	5.7	UT	1.5	2547	20.8	9.80	0.8	21.7	1845	3.8	16	70	11.2
Puhokio 2	IEJDB000O	39°49′50.48″S	176°58′23.36″E	9 March 2016	8.1	18.6	9.1	-	-	-	-	–0.2	-	-	-	2693	19.8	10.4	1.3	31.0	1929	2.7	25	52	25.9
Wairakau	IEJDB000Y	40°37′27.99″S	176°16′19.87″E	11 March 2016	-	-	-	-	-	-	-	-	-	-	-	-	-	-	bdl	bdl	33	1.7	8	313	28.4
Mangapakeha																									
Cone	IEJDB0016	40°54′17.0″S	176°00′50.8″E	25 June 2015	6.8	9.8	5.05	-	-	38.8	0.3	–0.1	29.0	C	2.6	2438	1.33	6.39	0.2	35.9	1664	3.8	5	50	3.3
Sulfide pool	IEJDB0019	40°54′17.0″S	176°00′50.8″E	25 June 2015	-	-	-	-	-	-	-	-	-	-	-	2463	3.34	6.22	0.3	35.1	1613	1.7	4	22	1.9
Main vent	IEJDB001A	40°54′17.0″S	176°00′50.8″E	25 June 2015	6.97	9.7	3.6	-	-	16.2	0.4	–0.3	-	-	-	2363	0.31	6.04	0.2	36.8	1577	7.1	11	104	8.3
Cone	IEJDB000V	40°54′17.0″S	176°00′50.8″E	11 March 2016	8.75	17.4	6	-	-	-	-	-	-	-	-	2488	12.1	6.80	0.4	37.6	1710	3.0	3	24	1.3
Small cone	IEJDB000W	40°54′17.0″S	176°00′50.8″E	11 March 2016	8.5	17.9	7.65	-	-	-	-	-	-	-	-	-	-	-	0.2	38.1	1649	2.5	3	27	2.0
Main vent	IEJDB000X	40°54′17.0″S	176°00′50.8″E	11 March 2016	7.91	17.7	5.78	-	-	37.9	1.2	–0.8	19.2	UT	2.8	2485	5.72	6.20	0.4	38.0	1555	4.4	6	44	3.4
Waikekino																									
1	IEJDB000S	41°15′2.34″S	175°49′45.12″E	10 March 2016	8.5	14.4	9.43	30.9	0.5	30.8	0.5	0.4	0.9	UT	4.8	3108	12.0	10.0	0.4	16.2	1976	6.2	9	33	3.5
								30.3	2.3	-	-	-	-	-	-										
2	IEJDB000T	41°15′2.34″S	175°49′45.12″E	10 March 2016	8.25	14.8	7.8	-	-	-	-	-	-	-	-	-	-	-	0.4	16.0	1997	5.3	6	27	2.9
3	IEJDB000U	41°15′2.34″S	175°49′45.12″E	10 March 2016	8.46	13.4	8.43	-	-	-	-	–0.6	–2.5	C	-	3140	6.68	10.6	0.4	17.4	1964	7.4	7	44	4.3

Notes: Concentrations are in mg/L. Replicate analyses of some samples are presented in multiple rows. Isotopic values are of boron, lithium, chlorine, and oxygen are relative to SRM951, L-SVEC, SMOC, and VSMOW, respectively. Given error for boron isotope analyses represents two standard deviations. Li isotope analyses were conducted in different labs (UT—University of Texas at Austin; C— Carnegie). IGSN—international geo sample number; wt avg—weighted average; bdl—below detection limit. If no value given (dash), then not analyzed.

limit (3σ) for the samples is 0.33 ng/ml for Br and 0.10 ng/ml for I. Accuracy is 5%–10% or better as based on analyses of a reference solution independently made from pure standards not used for calibration. Precision is around 2%–3% for I and 5%–10% for Br, as judged from the internal precision of all runs as well as from replicate analyses of two aliquots at the beginning and the end of the analytical session.

Cl, Li, B, and O Isotope Analyses

The chlorine isotope compositions of the waters were measured at UT-Austin using a Thermo Electron MAT 253 mass spectrometer and are reported in standard per mil notation versus standard mean ocean chloride (SMOC; $\delta^{37}Cl_{SMOC} = 0‰$). Cl isotope methods are based on Eggenkamp (1994). Analytical precision is ±0.2‰ (1 SD) based on the long-term precision of three seawater standards. Duplicate analyses are reported in Table 1, but all figures and discussion use average values.

The lithium concentrations and isotopic compositions of the waters were analyzed using the Nu Plasma HR multi-collector–ICP–MS (MC-ICP-MS) at the Department of Terrestrial Magnetism (DTM) at the Carnegie Institution of Washington (USA) and the Nu Plasma 3D at UT-Austin according to the method described in Teng et al. (2004). Waters were evaporated and taken up in 4M HCl for column chemistry at the University of Maryland (College Park, USA). These solutions were passed through three cation-exchange columns in order to separate Li for analysis. The samples were analyzed by standard bracketing using the L-SVEC standard. Samples were aspirated at ~50 µL/min at DTM and ~100 µL/min at UT-Austin. Results are reported as δ^7Li relative to the standard L-SVEC. Long-term reproducibility of Li isotope measurements is within ±1‰ (2σ) as determined by Teng et al. (2004), and verified through analysis of Li solution standards UMD-1 (+54.7‰) and IRMM-016 (+0.1‰) during each analytical run. The average δ^7Li value for all measurements of UMD-1 is 55.2‰ ± 0.9‰ (2 standard deviations [SD], $n = 5$) at DTM, and for IRMM-016 it is 0.1‰ ± 0.2‰ (2 SD, $n = 11$) at DTM and 0.2‰ ± 0.2‰ (2 SD, $n = 72$) at UT-Austin. Measured ^{7}Li voltages for samples are compared to the ^{7}Li voltage measured for the 50 ppb L-SVEC standard to determine the concentration of Li in solution and then adjusted for the mass of each sample powder dissolved to determine the rock Li concentration. This results in values for Li concentration with 2σ uncertainties of <±10% (Teng et al., 2006) for standard materials.

To evaluate potential inter-laboratory biases, a suite of 20 samples from this and other studies was analyzed at both DTM and UT-Austin (separate splits of same Li solution aliquot). The average offset between the DTM and UT-Austin analyses is only 0.04‰ (Fig. S1 in the Supplemental Material[1]), and the external reproducibility calculated from sample duplicate analyses is 0.61‰ (2 SD). This uncertainty incorporates analytical error at both DTM and UT-Austin, but does not account for error deriving from chemical separation and purification of lithium. To assess total procedural error, several lithium standards with matrices ranging from seawater to rhyolite were processed at the University of Maryland and analyzed at both DTM and UT-Austin. With the exception of one BVHO-2 analysis at DTM (measured δ^7Li = 2.63‰; accepted value = 4.70‰), the measured δ^7Li values of all geologic standards were within 1‰ of the accepted value (Fig. S2 [footnote 1]). Excluding the one outlier, the total external reproducibility is estimated at 0.75‰ (2 SD, $n = 8$). Inclusion of the outlier increases the estimated uncertainty to 1.2‰ (2 SD, $n = 9$).

The boron isotope compositions were determined at the Istituto di Geoscienze e Georisorse–Consiglio Nazionale delle Ricerche of Pisa (Italy) using a single-collector VG Isomass 54E positive thermal ionization mass spectrometer. Boron isotope composition of the sample is reported in the conventional delta-notation (δ^{11}B) as per mil (‰) deviation from the accepted composition of NIST SRM 951 (certified $^{11}B/^{10}B = 4.04362$; Catanzaro et al., 1970). Boron was separated from matrix by the ion-exchange chromatography procedure as described by Tonarini et al. (1997). The external reproducibility of B isotope composition is ±0.5‰, evaluated by repeated analyses of the NIST SRM 951 standard taken through the full chemistry.

The oxygen isotope compositions were measured at UT-Austin. Due to the highly saline nature of the samples, the waters were distilled under vacuum prior to analyses. Two milliliters (2 mL) of water was introduced into an Exetainer vial and flushed with 3000 ppm CO_2 in ultra-high purity helium. After samples were equilibrated for 24 h at 50 °C, headspace CO_2 was analyzed via continuous-flow mass spectrometry using at a GasBench II interfaced with a Thermo Electron MAT 253 mass spectrometer. All data are normalized to Vienna standard mean ocean water (VSMOW), using a four-point calibration of in-house standards which were themselves calibrated against VSMOW and Standard Light Antarctic Precipitation. Analytical precision is better than ±0.2‰ (1 SD).

RESULTS

Cation and anion concentrations have a large range along the length of the Hikurangi margin: Cl, 2400–16,000 mg/L; Br, 6–70 mg/L; I, 0.4–72 mg/L; Sr, 0.1–200 mg/L; B, 3–130 mg/L; Li, 0.1–13 mg/L; and Na, 33–6600 mg/L (Table 1; Table S1 [footnote 1]). Most elements show an overall decrease in concentration from north to south along the margin, as well as a noted concentration high in the central part of the margin at ~39°S (Fig. 2). Concentrations of Na, Cl, Sr, and Li in springs north of ~39°S are significantly higher than in springs south of ~39°S ($p < 0.05$; Mann-Whitney *U*-test, which evaluates the equality of means without assuming normally distributed variables, where values of $p < 0.05$ are typically considered significant). Br, B, and I concentrations are not significantly different in the north compared to the south, although the *p*-value for Br (0.068) is relatively low compared with those for B and I (0.5). Springs between 38°45′S and 39°15′S, at or near the central high concentrations, are not included in the statistical evaluation. The range in concentrations and overall trend are consistent with data from previous studies (Fehn et al., 2007; Giggenbach et al., 1995; Reyes et al., 2010). Br/Cl weight ratios range from 0.0025 to 0.005,

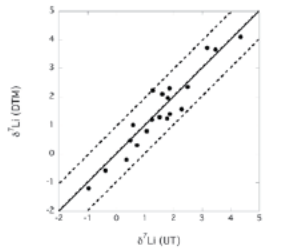

Supplemental Figure S1. A comparison of the Li isotope composition of samples run at both the University of Texas at Austin (UT) and the Department of Terrestrial Magnetism (DTM) at the Carnegie Institution of Washington (DTM). The solid line is the 1:1 line and the dashed lines are the ±1‰ lines.

[1]Supplemental Material. One table and three figures. Please visit https://doi.org/10.1130/GES02057.S1 or access the full-text article on www.gsapubs.org to view the Supplemental Material.

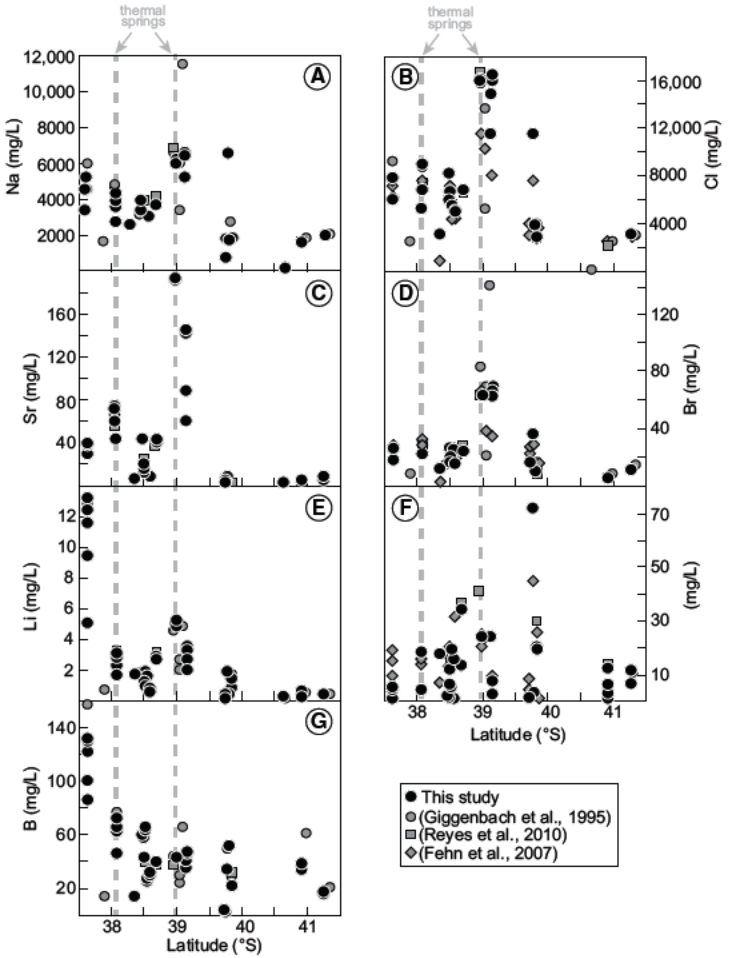

Figure 2. Cation and anion concentrations in forearc spring fluids along the length of the Hikurangi margin. Gray symbols show the previous data of Giggenbach et al. (1995), Fehn et al. (2007), and Reyes et al. (2010). Black symbols are data from this study. Gray dashed lines delineate the location of the two thermal springs, Te Puia and Morere.

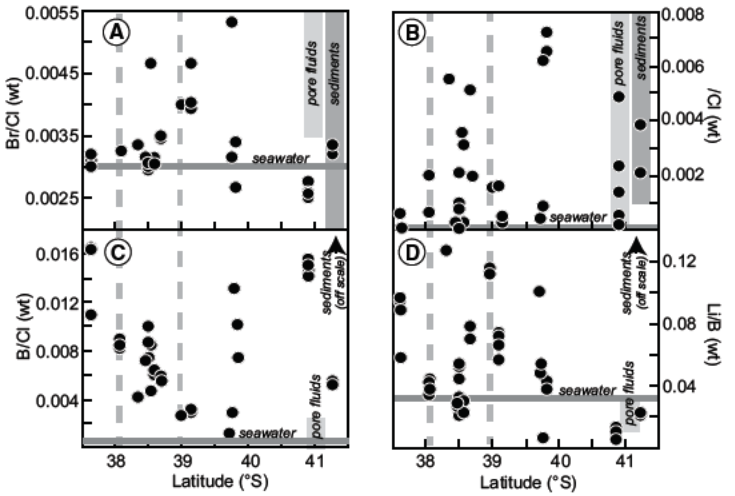

Figure 3. Halogen, boron, and lithium weight ratios of forearc spring fluids along the length of the Hikurangi margin. Seawater value and range of sedimentary pore fluid compositions are given for reference (Fehn et al., 2006, 2007; John et al., 2011; Kopf et al., 2000; Muramatsu et al., 2001; Wei et al., 2005). Ranges of Br/Cl and I/Cl values for sediments are from John et al. (2011). Sediments have high B/Cl and Li/B ratios based on the average values of the upper continental crust (0.05 and 1.2, respectively) (Rudnick and Gao, 2003). Gray dashed lines delineate the location of the two thermal springs, Te Puia and Morere.

I/Cl weight ratios from 0.00005 to 0.007, B/Cl weight ratios from 0.001 to 0.016, and Li/B weight ratios from 0.006 to 0.13 (Figs. 3 and 4). Note that the spring named Waitangi–oil is dominated by hydrocarbons. Data for Waitangi–oil are given in Table 1, but are not included in any figures or discussion given its distinctly different geochemistry compared to the other springs.

Values of δ^{37}Cl, δ^{11}B, and δ^{7}Li range from –1.3‰ to +0.4‰ (n = 36), 11.8‰ to 41.9‰ (n = 25), and –3.1‰ to +29.0‰ (n = 29), respectively (Table 1; Fig. 5). Despite the change in element concentration along the margin, there is no corresponding trend in the isotopic composition of the spring fluids. δ^{18}O values range from –7.1‰ to +6.5‰ (n = 18) (Table 1), consistent with previously reported δ^{18}O values of Hikurangi forearc springs (–4.6‰ to +7.1‰; Fig. S3 [footnote 1]) (Giggenbach et al., 1995; Reyes et al., 2010).

Based on comparison of these data with data from the same springs in past studies, there is limited variability in cation and anion concentrations through time (Fig. 2). We also sampled some springs twice in a nine-month period or three times in a two-year period and observed little change in cation and anion chemistry (Table 1; sampling date given). In addition, most discharge sites within a given spring system have similar cation and anion concentrations, although there is variability at some sites (e.g., Otopotehetehe, Te Puia) (Table 1; Fig. 2). No previously published Cl, B, or Li isotope data exist on these springs for comparison. Based on our work, there is no shift in the Cl, B, or Li isotope composition of the springs during the two-year sampling period, and most discharge sites within a given spring system have relatively constant δ^{37}Cl, δ^{11}B, and δ^{7}Li values (Table 1). However, two spring systems, Mahia and Mangapakeha, display large intra-spring system variability in δ^{11}B and δ^{7}Li values (Table 1). For example, three different discharge sites sampled at Mahia in 2016 have δ^{11}B values ranging from 23.1‰ to 37.7‰ and δ^{7}Li values ranging from –2.3‰ to +7.3‰.

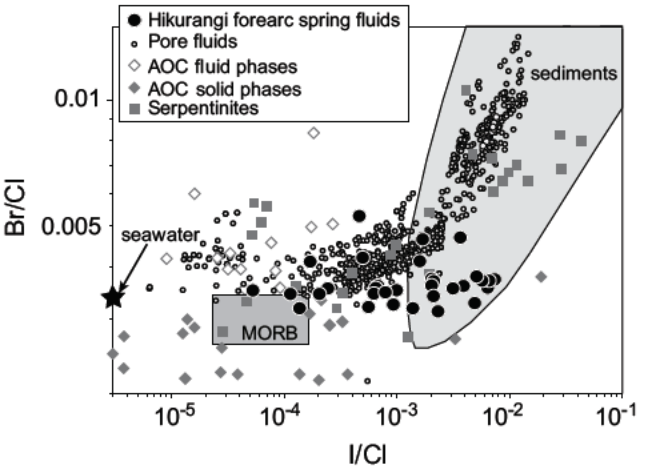

Figure 4. Br/Cl versus I/Cl ratios of Hikurangi forearc fluids (black circles). Halogen ratios of sedimentary pore fluids are from Fehn et al. (2006, 2007) and Muramatsu et al. (2001) and references therein. Sediment data are from John et al. (2011). Serpentinite data are from Kendrick et al. (2013). Altered oceanic crust (AOC) data are from Chavrit et al. (2016). Mid-ocean ridge basalt (MORB) data are from Jambon et al (1995) and Kendrick et al (2012a, 2012b). Figure modified from Kendrick et al. (2013).

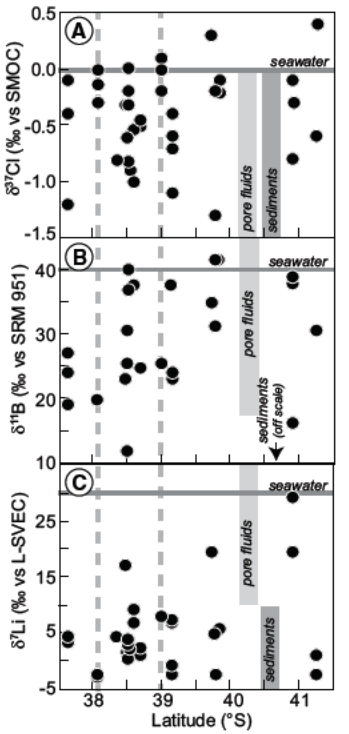

Figure 5. Chlorine, boron, and lithium isotope compositions of forearc spring fluids along the length of the Hikurangi margin. Values of seawater, sedimentary pore fluids, and marine sediments are given for reference (Barnes and Sharp, 2017; Deyhle and Kopf, 2002; Kopf et al., 2000; Palmer and Swihart, 2002; Tomascak et al., 2016; You et al., 1996). Gray dashed lines delineate the location of the two thermal springs, Te Puia and Morere.

DISCUSSION

Volatile Source

Some Li, Cl, and B can be incorporated into secondary minerals (e.g., zeolites, clays, chlorite, biotite, actinolite) during fluid-rock interaction, but in general, experimental and empirical data show that at temperatures <~150 °C, limited amounts of Li, Cl, and B are removed or added to the fluid either due to formation of secondary minerals or leaching of the host rock, respectively (e.g., Berger et al., 1988; James et al., 2003; Reyes and Trompetter, 2012; Seyfried et al., 1998, 1984). For Li, some experimental work has suggested that it can be released into the fluid phase with increasing temperatures from 25 to 250 °C despite the production of clay minerals (Millot et al., 2010), and at lower temperatures (<40 °C), B may be removed from the fluid by absorption onto clays (e.g., Keren and Mezuman, 1981; Palmer et al., 1987). Estimated subsurface temperatures for Hikurangi forearc cold and thermal springs are all <120 °C using K/Mg, K/Na, and silica geothermometry (Reyes et al., 2010), therefore modification of elemental ratios via fluid-rock interaction is thought to be limited, but we acknowledge that some modification is possible, particularly for lithium. More modification of elemental ratios is expected in the higher-temperature systems of Te Puia and Morere, which are highlighted in Figures 2, 3, and 5. To our knowledge, there are no published Cl, Li, or B isotope data for the subducting sediments at the Hikurangi trench or for the underlying rocks in the Hikurangi forearc, therefore compositional estimates for potential reservoirs are made based on global data sets.

Bromine/chlorine (Br/Cl) weight ratios in the forearc springs range from ~0.0025 to 0.005, similar to seawater (0.003) and marine sedimentary pore fluid values (0.0035–0.009) (Fehn et al., 2006, 2007; Muramatsu et al., 2001) (Figs. 3 and 4). I/Cl weight ratios span a large range from ~0.00005 to 0.007, overlapping with values of seawater, marine sedimentary pore fluids, and marine sediments (Fehn et al., 2006, 2007; John et al., 2011; Muramatsu et al., 2001) (Figs. 3 and 4). In contrast, B/Cl weight ratios (0.001–0.016) of the spring fluids are significantly higher than the seawater value of 0.00025. B/Cl weight ratios of marine sedimentary pore fluids range from 0.00009 to 0.002 (most values higher than that of seawater) (Kopf et al., 2000; Wei et al., 2005), overlapping with those of some spring fluids. The high boron concentrations in the spring fluids suggest the addition of boron, likely from either subducting sediments or local sediments within the forearc. Li/B weight ratios of the spring fluids range from 0.006 to 0.13, with most values higher than that of seawater (0.035). Sedimentary pore fluids have Li/B values of 0.01–0.9, with most values <0.03

(Kopf et al., 2000). High Li/B ratios in forearc fluids have previously been interpreted as being due to leaching of Li from the local rock (Giggenbach et al., 1995). Recent work on a prograde metasedimentary suite shows that little Li is lost from the subducting slab during dehydration reactions to depths of 40 km (Penniston-Dorland et al., 2012), supporting the interpretation that addition of Li may be locally derived rather than sourced from subducting sediments. Previous work interpreted higher $\delta^{18}O$ and δD values of forearc waters, compared to those of local groundwater, as indicating some contribution of fluids released from subducting dehydrating sediments or subducting sedimentary pore fluids with a fluid component derived from clay dehydration (Giggenbach et al., 1995; Reyes et al., 2010). Given the larger range of $\delta^{18}O$ values compared to δD values of the samples, $\delta^{18}O$ values are plotted relative to I/Cl, B/Cl, and Li/B (Figs. 6A–6C). Higher $\delta^{18}O$ values indicate a greater component of sedimentary-derived fluid. No strong correlations are observed between $\delta^{18}O$ values and I/Cl, B/Cl, and Li/B (Figs. 6A–6C), however if the Raukawa sample is ignored, the correlation between $\delta^{18}O$ values and Li/B is marginally significant (*F*-test; $p = 0.059$) suggesting some contribution from sediment-derived Li. In sum, based on elemental ratios alone, halogens, B, and Li are likely sourced from shallow recycling of seawater and marine sedimentary pore fluids, possibly with some contribution from local fluid-rock interaction. Chlorine, lithium, and boron isotope data are used to further evaluate source of these elements.

Previous work on the chlorine isotope composition of thermal waters (Yellowstone, western United States; Iceland; Indonesia; Cascadia, North American Pacific coast; Taupo Volcanic Zone, New Zealand) reports values ranging from ~−1‰ to ~+2‰, interpreted to reflect magmatic input and/or leaching of Cl from the host rock during water-rock interaction (Bernal et al., 2014; Cullen et al., 2015; Eggenkamp, 1994; Li et al., 2015; Stefánsson and Barnes, 2016; Zhang et al., 2004). Given the low temperature of the cold springs from the Hikurangi margin compared to these previous studies, it is likely that leaching of Cl from host rock is limited. The $\delta^{37}Cl$ values of the Hikurangi forearc fluids range from −1.3‰ to +0.4‰ (average = −0.4‰ ± 0.4‰) and show no trend along the length of the margin (Fig. 5). Seawater has a $\delta^{37}Cl$ value of 0‰ by definition (Kaufmann et al., 1984) and is isotopically homogeneous (Godon et al., 2004b). Marine sedimentary pore fluids range from −7.8‰ to +0.3‰, with the vast majority of samples being negative (Bonifacie et al., 2007; Godon et al., 2004a; Hesse et al., 2000; Ransom et al., 1995; Spivack et al., 2002). The range in $\delta^{37}Cl$ values of the forearc fluids (−1.3‰ to +0.4‰) suggests contributions from both seawater and sedimentary pore fluids. However, based on the chlorine isotope compositions alone, the dehydration of marine sediments, which have negative $\delta^{37}Cl$ values (down to −2.5‰) (Barnes et al., 2008, 2009), cannot be discounted as a chlorine source. Previous work shows no Cl isotope fractionation during metamorphic devolatilization of sedimentary rocks (Selverstone and Sharp, 2015), and therefore fluids released from dehydrating sediments should reflect their source composition. The lack of correlation between $\delta^{37}Cl$ and $\delta^{18}O$ values (Fig. 6F), as well as the lack of correlation between $\delta^{37}Cl$ values and I/Cl and Br/Cl ratios (Figs. 7A–7B) suggests that dehydrating marine sediments are not a significant Cl source. However, given the large possible range of $\delta^{37}Cl$ values and I/Cl and Br/Cl ratios for marine sediments, a distinct correlation may not occur.

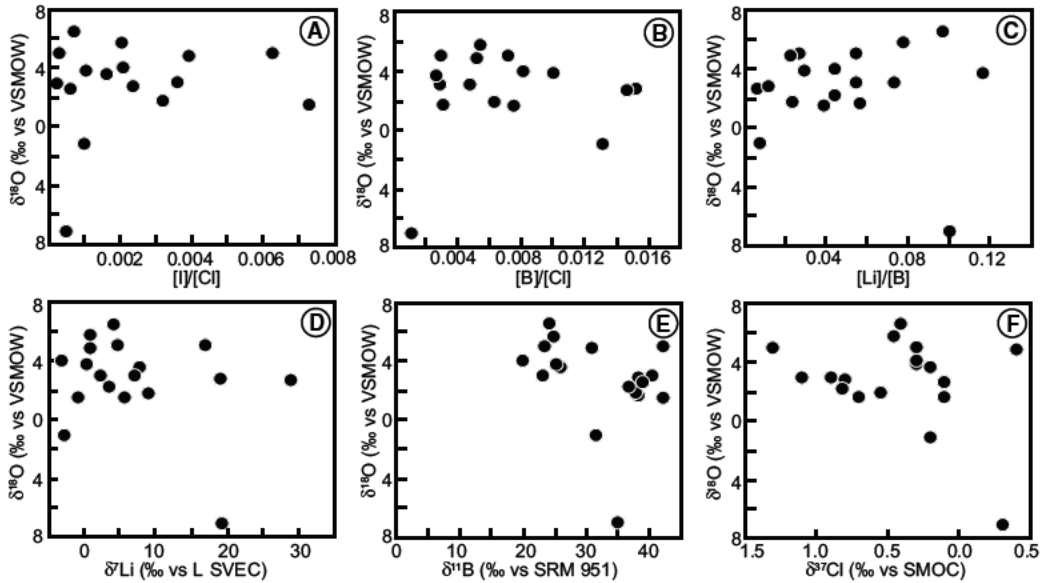

Figure 6. Oxygen isotope compositions of Hikurangi forearc spring waters compared to I/Cl, B/Cl, and Li/B weight ratios and Li, B, and Cl isotope compositions. All data are from this study.

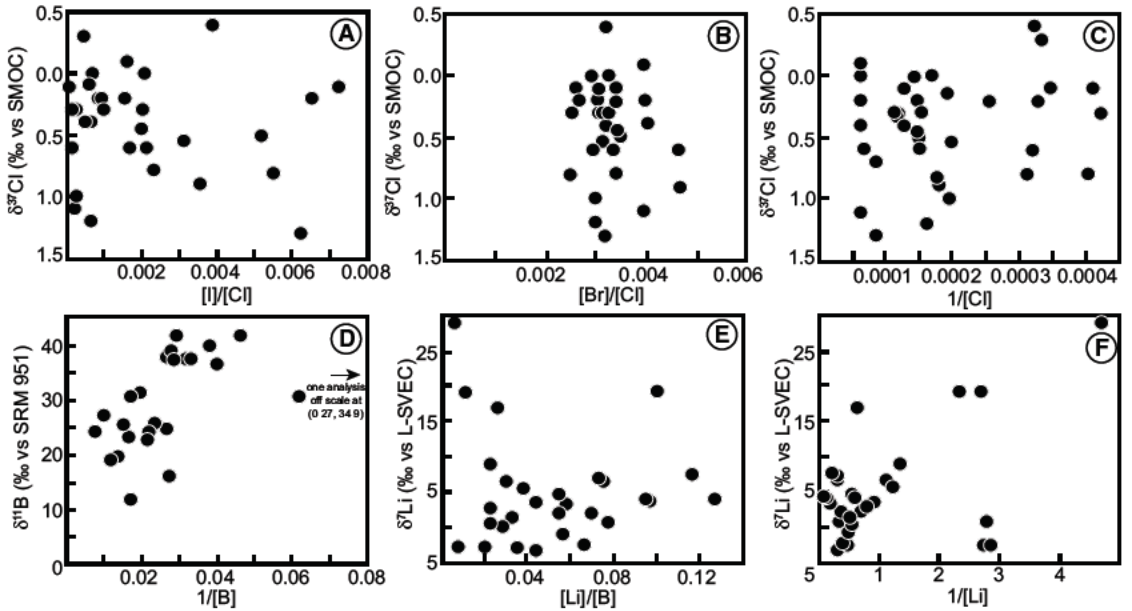

Figure 7. Li, B, and Cl isotope compositions of Hikurangi forearc springs waters compared to various elemental weight ratios of the same samples.

The boron isotope composition of geothermal fluids tends to show little variation with temperature or concentration of major elements (with the exception of Cl) (e.g., Millot and Négrel, 2007; Musashi et al., 1988; Palmer and Sturchio, 1990). Due to these observations and the relatively incompatible behavior of boron, B isotope geochemistry has been used to determine the source of B in hydrothermal fluids (Aggarwal et al., 2000, 2003; Millot et al., 2012; Millot and Négrel, 2007; Musashi et al., 1988; Palmer and Sturchio, 1990). $\delta^{11}B$ values of the Hikurangi forearc waters range from 11.8‰ to 41.9‰ (average = 29.7‰ ± 8.5‰) with no isotopic trend along the margin. These values are largely consistent with the values for seawater (39.6‰) and marine sedimentary pore fluids (>~17‰) (Deyhle and Kopf, 2002; Kopf et al., 2000; You et al., 1996, 1993). With increasing temperature during subduction, ^{10}B is preferentially desorbed from clays, leading to increasing boron concentration and decreasing $\delta^{11}B$ values documented in sedimentary pore fluids as well as in mud volcanoes (You et al., 1996). Recent modeling work suggests that at non-accretionary margins, which receive less incoming insulating sediments, like the northern Hikurangi, boron desorption and fractionation lead to higher concentrations of boron and lower $\delta^{11}B$ values in the pore fluids (Saffer and Kopf, 2016). If the Raukawa sample is ignored (off-scale point in Fig. 7D), then the correlation between 1/[B] and B isotope composition of the forearc springs is significant (Fig. 7D; *F*-test; $p = 0.004$); however, the trend is no longer significant if all data are included. In addition, B concentrations and $\delta^{11}B$ values are not significantly different in the north compared to the south (see Results section above). Instead, given the intra-spring boron isotopic variability, it is likely that the $\delta^{11}B$ values reflect some local absorption and desorption effects or minor interaction with host greywacke, for which a negative $\delta^{11}B$ value between –3.9‰ and –3.1‰ is assumed but not measured (Aggarwal et al., 2003). Such intra-spring isotopic variability is well documented at Mangapakeha. In 2015, the main vent had a $\delta^{11}B$ value of 16.2‰, whereas fluids from a nearby small cone had a $\delta^{11}B$ value of 38.8‰. In 2016, the main vent had a $\delta^{11}B$ value of 37.9‰. Although high B/Cl weight ratios of Mangapakeha fluids suggest an additional source of boron, high $\delta^{11}B$ values in the same samples suggest limited contribution of B from dehydrating sediments from the subducting slab or leached from local sediments, as sediments typically have negative $\delta^{11}B$ values of about –10‰ to ~0‰ (Palmer and Swihart, 2002). Experimental data suggest that B isotopes may fractionate during dehydration reactions, with fluid being enriched in ^{11}B by up to 30‰ with respect to clay at 25 °C (Wunder et al., 2005). However, even with such potentially large isotopic fractionation, the high $\delta^{11}B$ values (>30‰) are unlikely to be explained by fluids released from sediments.

Overall, the highly positive $\delta^{7}Li$ values (>+10‰) of the Hikurangi forearc fluids are consistent with a seawater and/or marine sedimentary pore fluid source (Fig. 5). Seawater has a $\delta^{7}Li$ value of +31‰, and sedimentary pore fluids have a large range in $\delta^{7}Li$ values from ~+10‰ to +45‰ (Tomascak et al., 2016, and references therein). The majority of the forearc fluids have $\delta^{7}Li$ values <+10‰ and are interpreted to represent local modification via interaction with host sediments and greywackes (sedimentary materials have $\delta^{7}Li$ values between ~–5‰ and +10‰; Tomascak et al., 2016, and references therein). Modeling of Li behavior during equilibrium fluid flow at higher temperatures in a paleo–accretionary wedge

(Otago Schist; Qiu et al., 2011) found that fluids with low Li concentrations (such as the waters of this study) would not retain the isotopic composition of their source. Rather the fluids may pick up the isotopic composition of the sedimentary rocks of the accretionary prism while traveling through them.

As discussed above, the behavior of lithium in hydrothermal systems is not well understood. Most hydrothermal experiments on sediments and basaltic glass show that little Li is released into solution at low temperatures (<~150 °C to 250 °C), but is lost to solution at higher temperatures (~350 °C) due to the breakdown of clay minerals and zeolites (e.g., Berger et al., 1988; James et al., 2003; Seyfried et al., 1998), suggesting limited modification in low-temperature systems. However, some experimental work has demonstrated an increase in Li concentration and decrease in δ^7Li value of the fluid during fluid-rock interaction with increasing temperature from 25 to 250 °C (Millot et al., 2010). That work suggested that variations in Li concentration and δ^7Li values can occur due to the competing effects of mineral dissolution and the precipitation of secondary minerals, which are more pronounced at higher temperature. The cold springs on the Hikurangi margin have δ^7Li values ranging from –2.6‰ to +29.0‰, whereas the thermal springs of Te Puia and Morere have δ^7Li values of –3.1‰ to –2.6‰ and of +7.8‰, respectively, indicating that there is not a direct relationship between δ^7Li values and temperature. However, it is interesting to note that the higher δ^7Li values are found in the cold springs. The interpretation of lowering of δ^7Li values due to fluid-rock interaction and addition of Li leached from the host rock implies a correlation between decreasing δ^7Li values and decreasing values of 1/Li, which are strongly correlated ($p = 2.5 \times 10^{-7}$; *F*-test; Fig. 7F) if values from Kahuranaki and Waikekino are ignored.

Diffusion of Li is another process that may contribute to variations in δ^7Li values. Lithium isotopes undergo kinetic fractionation during diffusion due to the faster diffusion of ^{6}Li compared to ^{7}Li, resulting in variations in δ^7Li values (e.g., Richter et al., 2006). Diffusion could induce isotopic fractionation during interaction between ascending fluids and wall rock due to Li diffusion assisted by a grain-boundary fluid (cf. Qiu et al., 2011). Li diffusion out of leach layers developed around minerals during mineral dissolution could also induce isotopic fractionation (e.g., Verney-Carron et al., 2011). This phenomenon was more pronounced during early stages of leaching, suggesting that the extent of fluid-rock interaction plays a role. The variability observed in some springs in this study, such as Mahia, may represent localized diffusive processes of either of these types.

Although Cl, B, and Li are all FMEs, their concentrations in a fluid and their isotopic composition in the fluid may be modified by fluid-rock interaction, with lithium being the most modified via incorporation in secondary minerals and kinetic fractionation, and chlorine the least modified. Therefore, although all three isotopic systems can be used to trace fluids, the three elements do not act in concert. The Li, Cl, and B isotope compositions of the Hikurangi margin fluids do not correlate with each other (Fig. 8), demonstrating that the isotopic compositions of the fluids do not simply reflect the mixing of different amounts of seawater. Instead, the differing behavior of the three elements leads to minor modifications to the isotopic systems as they interact with the upper plate during their upward ascent.

Role of the Upper Plate in Controlling Forearc Spring Fluid Chemistry

Halogen weight ratios, δ^{37}Cl values, and δ^{11}B values of the Hikurangi forearc fluids largely suggest that the fluids are dominated by shallowly expelled seawater and sedimentary pore fluids, with some sediment contribution, particularly in the case of lithium. It is likely that the sediment contribution is from local fluid-rock interaction in the accretionary wedge, as has also been proposed for high concentrations of iodine (Fehn and Snyder, 2003; Fehn et al., 2007) and the lithium isotope compositions (Qiu et al., 2011), rather than from dehydrating sediments in the subducting slab. Previous researchers have suggested some contribution (20%–55%) of water from the dehydration of subducting clays to the forearc fluids based on oxygen and hydrogen isotope data (Giggenbach et al., 1995); however, Cl, Li, and B ratios and isotope compositions show no strong correlations with δ^{18}O values, implying that these elements are minimally sourced by dehydrating subducting sediments (Fig. 6). Weak correlations between δ^{18}O values and Li/B may suggest the addition of some Li from local sedimentary rock. Despite the evidence for limited variation in FME source composition along the margin, there is a decrease in the absolute concentration of most FMEs from north to south and distinct concentration highs at ~39°S.

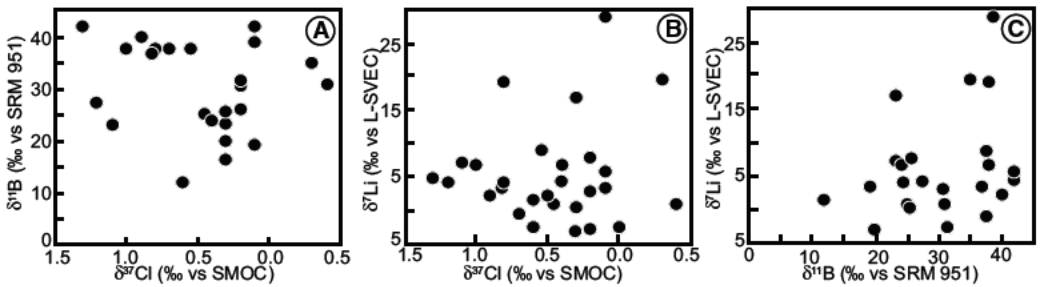

Figure 8. Plots of Cl, B, and Li isotope compositions of Hikurangi forearc spring waters.

Previous researchers have speculated that this decrease in concentration is due to a lower volume of subducted sediments or a lower volume of subducted water rising through the overlying crust in the south (Reyes et al., 2010). Although it has been shown that the sediment thickness on the downgoing plate is significantly greater in the south compared to the north (Lewis et al., 1998), seismic tomographic data suggest sediment subduction and/or underplating at the central and northern sections of the North Island where the margin is erosional, in contrast to the smaller amount of sediment subduction and/or underplating at the southern end of the island where a large accretionary prism is developed (e.g., Eberhart-Phillips and Bannister, 2015; Eberhart-Phillips et al., 2005). Yet, seismic reflection data show subducted and underplated sediment underneath the southern portion of the Hikurangi margin (Barker et al., 2009; Henrys et al., 2013). Therefore, it is unclear how much sediment subduction and/or underplating actually vary along the length of the Hikurangi margin (Wallace et al., 2009). Although the geochemical data presented in this work cannot definitively rule out a sedimentary component, as a whole they consistently indicate seawater and pore-fluid sources without a change in the sedimentary component along the length of the margin. We suggest that the change in the FME concentrations along the margin is not controlled by changes in subduction parameters such as the amount of sediments subducting, but rather by fluid flux through the upper plate.

The northern Hikurangi subduction interface is dominated by steady, aseismic creep at shallow depths (<15 km) and weak interseismic coupling (Wallace et al., 2009). In contrast, the southern portion of the Hikurangi subduction interface has deep slow-slip events and exhibits stick-slip behavior (Wallace and Beavan, 2010; Wallace et al., 2009) (Fig. 1). Previous work has suggested that the tectonic stress regime (extensional versus transpressional) in the upper plate may influence structural permeability and fluid pressure within the upper plate, which in turn may exert an influence on the shift in seismic behavior along the Hikurangi margin (Fagereng and Ellis, 2009; Sibson and Rowland, 2003; Wallace et al., 2012). In the northern and central portions of the margin (north of ~40.5°S), the upper plate is undergoing extension, whereas, in the southern portion (south of ~40.5°S), the upper plate is undergoing compression in the forearc (Wallace et al., 2004). The extension in the northern and central sections increases the structural permeability of the upper plate, allowing for fluid escape along vertical hydrofractures and normal faults, possibly leading to relatively lower fluid pressure in the forearc. In contrast, the transpressional regime in the south promotes horizontal hydrofracture, decreasing the structural permeability of the upper plate, trapping fluids and potentially increasing the fluid pressure within the forearc (Fagereng and Ellis, 2009; Wallace et al., 2012) (Fig. 9). Seismic tomography that imaged the Rakaia–Haast Schist terrane in the upper plate in the south shows that it may act as an aquiclude for the subduction interface (Eberhart-Phillips et al., 2008). Higher fluid pressures within the upper plate reduce the frictional strength, resulting in a deeper brittle-viscous transition and the occurrence of stick-slip behavior to greater depths (Fagereng and Ellis, 2009).

The model described above and summarized in Figure 9 can explain the decrease in FME concentrations in spring fluids from north to south and the distinct highs near the center (~39°S) of the margin. Trapping of expelled seawater and pore fluids in the upper plate in the south would allow the fluids to become diluted by groundwater, decreasing the concentrations of FMEs discharging from the springs. For example, seawater has an average chloride concentration of 19,354 mg/L, compared to 40 mg/L in average groundwater (Graedel and Keene, 1996) and 0.53 mg/L reported for surface meteoric waters discharging from greywacke (Reyes et al., 2010), but the chlorine isotope composition of the spring fluid would still reflect the dominant seawater chloride source. Concentrations of Na (1.2 mg/L), Sr (0.03 mg/L), Li (<0.05 mg/L), B (0.38 mg/L), and I (<0.001 mg/L) are also low in surface meteoric waters discharging from greywacke (Reyes et al., 2010), and therefore can account for low concentrations of these elements in the south. In the northern part of the margin, the seawater and pore fluids would pass through the upper plate with less dilution by groundwater. The noted peaks in Cl, Na, and Sr concentrations at Morere and Mahia are consistent with previous observations (Giggenbach et al., 1995; Reyes et al., 2010). These high concentrations are not due solely to

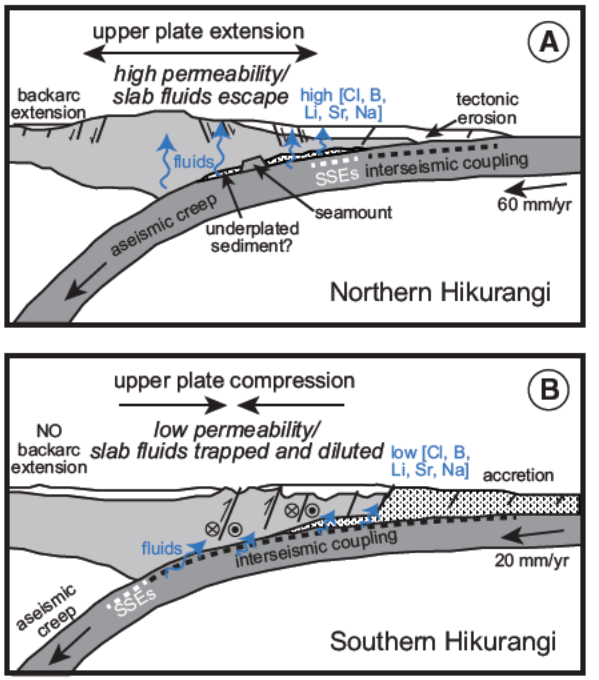

Figure 9. Schematic diagram showing upper-plate extension and escape of subduction-related fluids along normal faults in the northern Hikurangi margin (A), in contrast to upper-plate compression and entrapment and dilution of subduction-related fluids in the southern Hikurangi margin (B). Modified from Fagereng and Ellis (2009) and Wallace et al. (2012). SSEs—slow-slip events.

increased fluid-rock interaction at the thermal spring of Morere, as concentrations are similar or even higher in the Mahia cold-spring fluids. Giggenbach et al. (1995) interpreted the high R/R_A value of 3.35 at Morere to reflect a greater fluid pathway to the mantle wedge and the subducted component. Interestingly, Mahia has a much lower R/R_A value of 0.53 (Giggenbach et al., 1995); therefore, the high FME concentrations in the fluids are not necessarily coupled to high $^3He/^4He$ ratios in gases. Although the high $^3He/^4He$ ratios clearly demonstrate that some mantle component is present in the springs, we argue that the FME chemistry of the springs fluids largely reflects the structure of the upper plate.

Seismic tomographic and attenuation data show that more abundant, interconnected fluid is present in the northern and central portions of the upper plate of the Hikurangi subduction zone, compared to the south (Eberhart-Phillips et al., 2017, 2005, 2008). The parameter *Q* (the inverse of seismic attenuation) can be used as a proxy for fluid content. An increase in porosity and fluid pressure increases attenuation, and therefore decreases *Q*. Figure 10 shows *Qs* data, where *s* is for shear waves, for the Hikurangi margin at a depth of 8 km from Eberhart-Phillips et al. (2017), along with the location of the springs sampled for this study. The springs clearly correspond with regions of low *Qs* (high attenuation). In addition, springs with the highest concentrations of FMEs in the northern part of the margin are located in regions with some of the lowest *Qs* values. Whether or not the low *Qs* values in the north represent high fluid pressure in the upper plate (e.g., Eberhart-Phillips et al., 2017) or are simply a consequence of well-connected fluid-filled pathways (without significant overpressure) is currently unknown. Distinguishing between these two possibilities has important implications for the validity of the assertion that fluid pressure in the forearc (1) influences the depth to the brittle-viscous transition and (2) explains the distribution of locking versus aseismic creep at the Hikurangi margin (e.g., Fagereng and Ellis, 2009; Wallace et al., 2012).

Remarkably, more springs have been discovered and sampled in the northern and central portions of the margin than in the south. This does not exclude the presence of additional, undiscovered springs in the south, but tends to support the conclusion of a more permeable upper plate, with larger volumes of fluids emerging in the northern and central parts of the margin.

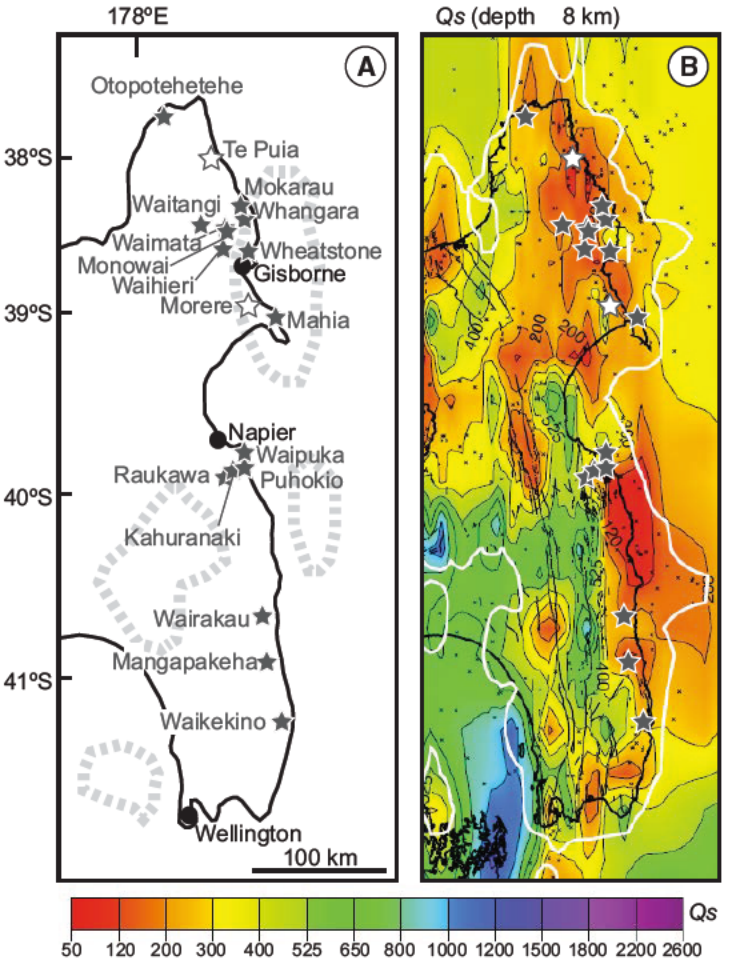

Figure 10. (A) Map from Figure 1 showing the location of sampled springs along the Hikurangi margin. Dashed gray areas show the location of slow-slip event (SSE) regions. (B) Map view of *Qs* (inverse of seismic attenuation for shear waves) data at a depth of 8 km. Data are from Eberhart-Phillips et al. (2017) and overlain with location of springs. White lines delineate limit of adequate resolution, and small cross symbols show location of hypocenters (see Eberhart-Phillips et al. [2017] for more details). Note that the spring locations tend to be located in areas of low *Qs*.

Implications for Volatile Flux through Subduction Zones

Most volatile and FME flux mass-balance calculations through subduction zones focus on inputs from the subducting slab and outputs from the volcanic front (e.g., Barnes et al., 2018; Fischer, 2008; Wallace, 2005). Volatile and FME fluxes through the forearc, including loss via spring systems, may be substantial, but are poorly constrained (e.g., Freundt et al., 2014; Shinohara, 2013; Taran, 2009; Völker et al., 2014), thereby making cycling estimates through subduction zones subject to large error. Pore fluid trapped in subducting sediments is estimated to represent 42% of the total water input into subduction zones (Jarrard, 2003). However, it is typically assumed that the majority of sedimentary pore fluids is expelled at shallow levels (<15 km) during subduction due to compaction (e.g., Jarrard, 2003; Kastner et al., 1991; Saffer and Tobin, 2011); therefore, contributions from pore fluids are ignored in mass-balance calculations through subduction zones. Our data suggest that chlorine and boron fluxed through the shallow portion of the forearc (<~15 km depth) are largely sourced from seawater and pore fluids, rather than from dehydration reactions within

the subducting slab, supporting this assumption. However, without additional constraints, we cannot conclude that no pore fluids make it past these shallow depths. Previous work based on the thickness of subducting and accreting sediment, initial and final porosity in accreted and subducted sediment, and clay content in sediment estimate that between ~20 and ~40 m^3 of fluid is discharged per meter length along the Hikurangi (or northern Hikurangi) margin per year, with the majority of this fluid derived from pore fluids via compaction (Ellis et al., 2015; Pecher et al., 2010; Townend, 1997). In order to calculate the percentage of pore fluid lost by 15 km depth, constraints on the actual fluid flux through onshore and offshore forearc springs, not just the predicted flux, must be known. To our knowledge, there are no integrated flux estimates based on measured fluid flow rates through the springs. However, first-order estimates can be made using the reported flow of ~3–9 L/s at the thermal springs (e.g., Pohatu et al., 2010). If we assume 0.5 L/s per spring, 250 onshore and offshore springs, and 800 km of margin, then ~5 m^3 of fluid is discharged per meter length per year along the Hikurangi margin. We acknowledge a large error on this estimate, but to a first order it is the same as the estimated pore-fluid release due to compaction, suggesting that most pore fluids are recycled through the shallow portion of the subduction zone. Future work monitoring fluid discharge through forearc springs is needed to better quantify the extent of elemental recycling through the shallow portion of the subduction zone.

In addition, integrated geochemical data sets of across forearc profiles from multiple subduction zones are needed to fully quantify volatile and FME loss, as well as their source, between the trench and the arc front. For example, boron concentrations consistently decrease from the forearc to the backarc across the Cascadia, Izu (offshore Japan), Kamchatka (northwest Pacific), and Kurile (northwest Pacific) subduction zones (Ishikawa and Nakamura, 1994; Ishikawa and Tera, 1997; Konrad-Schmolke et al., 2016; Leeman et al., 2004; Straub and Layne, 2002), with most of the boron estimated to be derived from the subducting slab (Straub and Layne, 2002). Savov et al. (2005) calculated that 79% of B is lost by 40 km depth, compared to 18% of Li, and Ishikawa and Tera (1997) suggested that up to 97% of B is lost in the forearc. A more complete understanding of the contribution of pore fluids versus slab-derived fluids across the entire forearc is needed to evaluate global geochemical cycles.

SUMMARY AND CONCLUSIONS

Spring fluids from the Hikurangi forearc show a decrease in Cl, Li, Sr, and Na concentrations from north to south along the margin. These changes in concentration raise the possibility that a shift in subduction parameters along strike may control the chemistry of the springs. Additionally, the change in seismic behavior along the margin from shallow aseismic creep in the north to stick slip in the south may be caused by a change in the fluid source from the dehydrating slab. However, new stable isotope data (Cl, Li, B) presented here demonstrate that there is no systematic change in fluid source along the margin. Most data can be explained by shallowly recycled seawater or sedimentary pore fluids, with some local modification by interaction with sediments. The data are consistent with a model of extension in the northern portion of the forearc allowing for escape of the fluids along normal faults and vertical hydrofractures, and trapping of fluids in the transpressional upper plate in the south resulting in dilution. In turn, the ability of the upper plate to trap fluids (or not) may influence fluid pressures in the upper plate, which could influence the depth to the brittle-viscous transition and the occurrence of aseismic creep versus stick-slip behavior (e.g., Fagereng and Ellis, 2009; Wallace et al., 2012). This work highlights the important role the upper plate plays in the development fluid pathways and geochemistry of spring fluids, and the potential influence of fluid pressure state within the upper plate on subduction-interface slip behavior. In addition, we confirm the previous assumption that seawater and sedimentary pore fluids are shallowly (<15 km) expelled during subduction. Future work is needed on across-forearc profiles in order to evaluate the shift in slab-derived fluid sources from shallow seawater and/or pore-fluid release to dehydration of mineral phases, as well as quantifying the FME output from the forearc and its contribution to global-scale elemental cycling.

ACKNOWLEDGMENTS

Thank you to the New Zealand landowners and the Iwi Council who generously allowed us to sample on their land. T. Mock, S. Shirey, R. Ash, S. Loewy, and A. Satkoski are thanked for their assistance with Li isotope analyses, N. Miller for assistance with cation analyses, P. Monien for the Br and I analyses, and D. Xu for oxygen isotope analyses. B. Andrew and J. Mering assisted with field work. The authors thank S. Ellis, A. Reyes, M. Reyners, and D. Eberhart-Phillips for helpful discussions, and W. Leeman for constructive comments on a previous version of this manuscript. R. Halama and an anonymous reviewer are thanked for their helpful reviews. This work was funded by U.S. National Science Foundation GeoPRISMS grant 1455432.

REFERENCES CITED

Aggarwal, J.K., Palmer, M.R., Bullen, T.D., Arnórsson, S., and Ragnarsdóttir, K.V., 2000, The boron isotope systematics of Icelandic geothermal waters: 1. Meteoric water charged systems: Geochimica et Cosmochimica Acta, v. 64, p. 579–585, https://doi.org/10.1016/S0016-7037(99)00300-2.

Aggarwal, J.K., Sheppard, D., Mezger, K., and Pernicka, E., 2003, Precise and accurate determination of boron isotope ratios by multiple collector ICP-MS: Origin of boron in the Ngawha geothermal system, New Zealand: Chemical Geology, v. 199, p. 331–342, https://doi.org/10.1016/S0009-2541(03)00127-X.

Barker, D.H.N., Sutherland, R., Henrys, S., and Bannister, S., 2009, Geometry of the Hikurangi subduction thrust and upper plate, North Island, New Zealand: Geochemistry, Geophysics, Geosystems, v. 10, Q02007, https://doi.org/10.1029/2008GC002153.

Barnes, J.D., and Sharp, Z.D., 2017, Chlorine isotope geochemistry, *in* Tang, F.-Z., Watkins, J., and Dauphas, N., eds., Measurements, Theories and Applications of Non-Traditional Stable Isotopes: Mineralogical Society of America, Reviews in Mineralogy and Geochemistry, v. 82, p. 345–378, https://doi.org/10.1515/9783110545630-010.

Barnes, J.D., Sharp, Z.D., and Fischer, T.P., 2008, Chlorine isotope variations across the Izu-Bonin-Mariana arc: Geology, v. 36, p. 883–886, https://doi.org/10.1130/G25182A.1.

Barnes, J.D., Sharp, Z.D., Fischer, T.P., Hilton, D.R., and Carr, M.J., 2009, Chlorine isotope variations along the Central American volcanic front and back arc: Geochemistry Geophysics Geosystems, v. 10, Q11S17, https://doi.org/10.1029/2009GC002587.

Barnes, J.D., Manning, C.E., Scambelluri, M., and Selverstone, J., 2018, Behavior of halogens during subduction zone processes, *in* Harlov, D., and Aranovich, L., eds., The Role of Halogens in Terrestrial and Extraterrestrial Geochemical Processes: Springer, p. 545–590, https://doi.org/10.1007/978-3-319-61667-4_8.

Barnes, P.M., Lamarche, G., Bialas, J., Henrys, S., Pecher, I., Netzeband, G.L., Greinert, J., Mountjoy, J.J., Pedley, K., and Crutchley, G., 2010, Tectonic and geological framework for gas hydrates and cold seeps on the Hikurangi subduction margin, New Zealand: Marine Geology, v. 272, p. 26–48, https://doi.org/10.1016/j.margeo.2009.03.012.

Berger, G., Schott, J., and Guy, C., 1988, Behavior of Li, Rb and Cs during basalt glass and olivine dissolution and chlorite, smectite and zeolite precipitation from seawater: Experimental investigations and modelization between 50° and 300°C: Chemical Geology, v. 71, p. 297–312, https://doi.org/10.1016/0009-2541(88)90056-3.

Bernal, N.F., Gleeson, S.A., Dean, A.S., Liu, X.M., and Hoskin, P., 2014, The source of halogens in geothermal fluids from the Taupo Volcanic Zone, North Island, New Zealand: Geochimica et Cosmochimica Acta, v. 126, p. 265–283, https://doi.org/10.1016/j.gca.2013.11.003.

Bonifacie, M., Monnin, C., Jendrzejewski, N., Agrinier, P., and Javoy, M., 2007, Chlorine stable isotopic composition of basement fluids of the eastern flank of the Juan de Fuca Ridge (ODP Leg 168): Earth and Planetary Science Letters, v. 260, p. 10–22, https://doi.org/10.1016/j.epsl.2007.05.011.

Bu, X.D., Wang, T.B., and Hall, G., 2003, Determination of halogens in organic compounds by high resolution inductively coupled plasma mass spectrometry (HR-ICP-MS): Journal of Analytical Atomic Spectrometry, v. 18, p. 1443–1451, https://doi.org/10.1039/b306570g.

Cashman, S.M., Kelsey, H.M., Erdman, C.F., Cutten, H.N., and Berryman, K.R., 1992, Strain partitioning between structural domains in the forearc of the Hikurangi subduction zone, New Zealand: Tectonics, v. 11, p. 242–257, https://doi.org/10.1029/91TC02363.

Catanzaro, E.J., Champion, C.E., Garner, E.L., Malinenko, G., Sappenfield, K.M., and Shields, K.M., 1970, Boric acid: Isotopic and assay standard reference materials: U.S. National Bureau of Standards Special Publication 260-17, 60 p.

Chavrit, D., Burgess, R., Sumino, H., Teagle, D.A.H., Droop, G., Shimizu, A., and Ballentine, C.J., 2016, The contribution of hydrothermally altered ocean crust to the mantle halogen and noble gas cycles: Geochimica et Cosmochimica Acta, v. 183, p. 106–124, https://doi.org/10.1016/j.gca.2016.03.014.

Chiaradia, M., Barnes, J.D., and Cadet-Voisin, S., 2014, Chlorine isotope variations across the Quaternary volcanic arc of Ecuador: Earth and Planetary Science Letters, v. 396, p. 22–33, https://doi.org/10.1016/j.epsl.2014.03.062.

Cullen, J.T., Barnes, J.D., Hurwitz, S., and Leeman, W.P., 2015, Halogen and chlorine isotope composition of thermal springs along and across the Cascadia arc: Earth and Planetary Science Letters, v. 426, p. 225–234, https://doi.org/10.1016/j.epsl.2015.06.052.

Darby, D., and Funnell, R.H., 2001, Overpressure associated with a convergent plate margin: East Coast Basin, New Zealand: Petroleum Geoscience, v. 7, p. 291–299, https://doi.org/10.1144/petgeo.7.3.291.

Davy, B., and Wood, R., 1994, Gravity and magnetic modelling of the Hikurangi Plateau: Marine Geology, v. 118, p. 139–151, https://doi.org/10.1016/0025-3227(94)90117-1.

Davy, B., Hoernle, K., and Werner, R., 2008, Hikurangi Plateau: Crustal structure, rifted formation, and Gondwana subduction history: Geochemistry, Geophysics, Geosystems, v. 9, Q07004, https://doi.org/10.1029/2007GC001855.

Deyhle, A., and Kopf, A., 2002, Strong B enrichment and anomalous $\delta^{11}B$ in pore fluids from the Japan Trench forearc: Marine Geology, v. 183, p. 1–15, https://doi.org/10.1016/S0025-3227(02)00186-X.

Eberhart-Phillips, D., and Bannister, S., 2015, 3-D imaging of the northern Hikurangi subduction zone, New Zealand: Variations in subducted sediment, slab fluids and slow slip: Geophysical Journal International, v. 201, p. 838–855, https://doi.org/10.1093/gji/ggv057.

Eberhart-Phillips, D., and Reyners, M., 2001, A complex, young subduction zone imaged by three-dimensional seismic velocity, Fiordland, New Zealand: Geophysical Journal International, v. 146, p. 731–746, https://doi.org/10.1046/j.0956-540x.2001.01485.x.

Eberhart-Phillips, D., Reyners, M., Chadwick, M., and Chiu, J.-M., 2005, Crustal heterogeneity and subduction processes: 3-D *Vp*, *Vp*/*Vs* and *Q* in the southern North Island, New Zealand: Geophysical Journal International, v. 162, p. 270–288, https://doi.org/10.1111/j.1365-246X.2005.02530.x.

Eberhart-Phillips, D., Reyners, M., Chadwick, M., and Stuart, G., 2008, Three-dimensional attenuation structure of the Hikurangi subduction zone in the central North Island, New Zealand: Geophysical Journal International, v. 174, p. 418–434, https://doi.org/10.1111/j.1365-246X.2008.03816.x.

Eberhart-Phillips, D., Bannister, S., and Reyners, M., 2017, Deciphering the 3-D distribution of fluid along the shallow Hikurangi subduction zone using *P*- and *S*-wave attenuation: Geophysical Journal International, v. 211, p. 1032–1045, https://doi.org/10.1093/gji/ggx348.

Eggenkamp, H.G.M., 1994, $\delta^{37}Cl$: The geochemistry of chlorine isotopes [Ph.D. thesis]: Utrecht, Universiteit Utrecht, 151 p.

Elliott, T., Thomas, A., Jeffcoate, A., and Niu, Y., 2006, Lithium isotope evidence for subduction-enriched mantle in the source of mid-ocean ridge basalts: Nature, v. 443, p. 565–568, https://doi.org/10.1038/nature05144.

Ellis, S., Fagereng, Å., Barker, D., Henrys, S., Saffer, D., Wallace, L., Williams, C., and Harris, R., 2015, Fluid budgets along the northern Hikurangi subduction margin, New Zealand: The effect of a subducting seamount on fluid pressure: Geophysical Journal International, v. 202, p. 277–297, https://doi.org/10.1093/gji/ggv127.

Fagereng, Å., and Ellis, S., 2009, On factors controlling the depth of interseismic coupling on the Hikurangi subduction interface, New Zealand: Earth and Planetary Science Letters, v. 278, p. 120–130, https://doi.org/10.1016/j.epsl.2008.11.033.

Fehn, U., and Snyder, G.T., 2003, Origin of iodine and ^{129}I in volcanic and geothermal fluids from the North Island of New Zealand: Implications for subduction zone processes, *in* Simmons, S.F., and Graham, I., eds., Volcanic, Geothermal, and Ore-Forming Fluids: Rulers and Witnesses of Processes within the Earth: Society of Economic Geologists Special Publication 10, p. 159–170.

Fehn, U., Lu, Z., and Tomaru, H., 2006, Data report: $^{129}I/I$ ratios and halogen concentrations in pore water of Hydrate Ridge and their relevance for the origin of gas hydrates: A progress report, *in* Tréhu, A.M., Bohrmann, G., Torres, M.E., and Colwell, F.S., eds., Proceedings of the Ocean Drilling Program, Scientific Results, Volume 204: College Station, Texas, Ocean Drilling Program, 25 p., https://doi.org/10.2973/odp.proc.sr.204.107.2006.

Fehn, U., Snyder, G.T., and Muramatsu, Y., 2007, Iodine as a tracer of organic material: ^{129}I results from gas hydrate systems and fore arc fluids: Journal of Geochemical Exploration, v. 95, p. 66–80, https://doi.org/10.1016/j.gexplo.2007.05.005.

Fischer, T.P., 2008, Fluxes of volatiles (H_2O, CO_2, N_2, Cl, F) from arc volcanoes: Geochemical Journal, v. 42, p. 21–38, https://doi.org/10.2343/geochemj.42.21.

Freundt, A., Grevemeyer, I., Rabbel, W., Hansteen, T.H., Hensen, C., Wehrmann, H., Kutterolf, S., Halama, R., and Frische, M., 2014, Volatile (H_2O, CO_2, Cl, S) budget of the Central American subduction zone: International Journal of Earth Sciences, v. 103, p. 2101–2127, https://doi.org/10.1007/s00531-014-1001-1.

Fūri, E., Hilton, D.R., Tryon, M.D., Brown, K.M., McMurtry, G.M., Brückmann, W., and Wheat, C.G., 2010, Carbon release from submarine seeps at the Costa Rica fore arc: Implications for the volatile cycle at the Central America convergent margin: Geochemistry Geophysics Geosystems, v. 11, Q04S21, https://doi.org/10.1029/2009GC002810.

Giggenbach, W.F., Sano, Y., and Wakita, H., 1993, Isotopic composition of helium, CO_2 and CH_4 contents in gases produced along the New Zealand part of a convergent plate boundary: Geochimica et Cosmochimica Acta, v. 57, p. 3427–3455, https://doi.org/10.1016/0016-7037(93)90549-C.

Giggenbach, W.F., Stewart, M.K., Sano, Y., Goguel, R.L., and Lyon, G.L., 1995, Isotopic and chemical composition of solutions and gases from the East Coast accretionary prism, New Zealand, *in* Isotope and Geochemical Techniques Applied to Geothermal Investigations: International Atomic Energy Agency TECDOC 788, p. 209–231.

Godon, A., Jendrzejewski, N., Castrec-Rouelle, M., Dia, A., Pineau, F., Boulègue, J., and Javoy, M., 2004a, Origin and evolution of fluids from mud volcanoes in the Barbados accretionary complex: Geochimica et Cosmochimica Acta, v. 68, p. 2153–2165, https://doi.org/10.1016/j.gca.2003.08.021.

Godon, A., Jendrzejewski, N., Eggenkamp, H.G.M., Banks, D.A., Ader, M., Coleman, M.L., and Pineau, F., 2004b, A cross-calibration of chlorine isotopic measurements and suitability of seawater as the international reference material: Chemical Geology, v. 207, p. 1–12, https://doi.org/10.1016/j.chemgeo.2003.11.019.

Graedel, T.E., and Keene, W.C., 1996, The budget and cycle of Earth's natural chlorine: Pure and Applied Chemistry, v. 68, p. 1689–1697, https://doi.org/10.1351/pac199668091689.

Henrys, S., Wech, A., Sutherland, R., Stern, T., Savage, M., Sato, H., Mochizuki, K., Iwasaki, T., Okaya, D., Seward, A., Tozer, B., Townend, J., Kurashimo, E., Iidaka, T., and Ishiyama, T., 2013, SAHKE geophysical transect reveals crustal and subduction zone structure at the southern Hikurangi margin, New Zealand: Geochemistry Geophysics Geosystems, v. 14, p. 2063–2083, https://doi.org/10.1002/ggge.20136.

Hesse, R., Frape, S.K., Egeberg, P.K., and Matsumoto, R., 2000, Stable isotope studies (Cl, O, and H) of interstitial waters from Site 997, Blake Ridge gas hydrate field, West Atlantic, *in* Paull, C.K., Matsumoto, R., Wallace, P.J., and Dillon, W.P., eds., Proceedings of the Ocean Drilling Program, Scientific Results, Volume 164: College Station, Texas, Ocean Drilling Program, p. 129–137, https://doi.org/10.2973/odp.proc.sr.164.238.2000.

Ishikawa, T., and Nakamura, E., 1994, Origin of the slab component in arc lavas from across-arc variation of B and Pb isotopes: Nature, v. 370, p. 205–208, https://doi.org/10.1038/370205a0.

Ishikawa, T., and Tera, F., 1997, Source, composition and distribution of the fluid in the Kurile mantle wedge: Constraints from across-arc variations of B/Nb and B isotopes: Earth and Planetary Science Letters, v. 152, p. 123–138, https://doi.org/10.1016/S0012-821X(97)00144-1.

Jambon, A., Deruelle, B., Dreibus, G., and Pineau, F., 1995, Chlorine and bromine abundance in MORB: The contrasting behaviour of the Mid-Atlantic Ridge and East Pacific Rise and implications for chlorine geodynamic cycle: Chemical Geology, v. 126, p. 101–117, https://doi.org/10.1016/0009-2541(95)00112-4.

James, R.H., Allen, D.E., and Seyfried, W.E., Jr., 2003, An experimental study of alteration of oceanic crust and terrigenous sediments at moderate temperatures (51 to 350°C): Insights as to chemical processes in near-shore ridge-flank hydrothermal systems: Geochimica et Cosmochimica Acta, v. 67, p. 681–691, https://doi.org/10.1016/S0016-7037(02)01113-4.

Jarrard, R.D., 2003, Subduction fluxes of water, carbon dioxide, chlorine, and potassium: Geochemistry, Geophysics, Geosystems, v. 4, 8905, https://doi.org/10.1029/2002GC000392.

John, T., Layne, G.D., Haase, K.M., and Barnes, J.D., 2010, Chlorine isotope evidence for crustal recycling into the Earth's mantle: Earth and Planetary Science Letters, v. 298, p. 175–182, https://doi.org/10.1016/j.epsl.2010.07.039.

John, T., Scambelluri, M., Frische, M., Barnes, J.D., and Bach, W., 2011, Dehydration of subducting serpentinite: Implications for halogen mobility in subduction zones and the deep halogen cycle: Earth and Planetary Science Letters, v. 308, p. 65–76, https://doi.org/10.1016/j.epsl.2011.05.038.

Kastner, M., Elderfield, H., and Martin, J.B., 1991, Fluids in convergent margins: What do we know about their composition, origin, role in diagenesis and importance for oceanic chemical fluxes?: Philosophical Transactions of the Royal Society of London A, v. 335, p. 243–259, https://doi.org/10.1098/rsta.1991.0045.

Kaufmann, R., Long, A., Bentley, H., and Davis, S., 1984, Natural chlorine isotope variations: Nature, v. 309, p. 338–340, https://doi.org/10.1038/309338a0.

Kendrick, M.A., Woodhead, J.D., and Kamenetsky, V.S., 2012a, Tracking halogens through the subduction cycle: Geology, v. 40, p. 1075–1078, https://doi.org/10.1130/G33265.1.

Kendrick, M.A., Kamenetsky, V.S., Phillips, D., and Honda, M., 2012b, Halogen (Cl, Br, I) systematics of mid-ocean ridge basalts: A Macquarie Island case study: Geochimica et Cosmochimica Acta, v. 81, p. 82–93.

Kendrick, M.A., Honda, M., Pettke, T., Scambelluri, M., Phillips, D., and Giuliani, A., 2013, Subduction zone fluxes of halogens and noble gases in seafloor and forearc serpentinites: Earth and Planetary Science Letters, v. 365, p. 86–96, https://doi.org/10.1016/j.epsl.2013.01.006.

Keren, R., and Mezuman, U., 1981, Boron adsorption by clay minerals using a phenomenological equation: Clays and Clay Minerals, v. 29, p. 198–204, https://doi.org/10.1346/CCMN.1981.0290305.

Konrad-Schmolke, M., Halama, R., and Manea, V.C., 2016, Slab mantle dehydrates beneath Kamchatka—Yet recycles water into the deep mantle: Geochemistry Geophysics Geosystems, v. 17, p. 2987–3007, https://doi.org/10.1002/2016GC006335.

Kopf, A., Deyhle, A., and Zuleger, E., 2000, Evidence for deep fluid circulation and gas hydrate dissociation using boron and boron isotopes of pore fluids in forearc sediments from Costa Rica (ODP Leg 170): Marine Geology, v. 167, p. 1–28, https://doi.org/10.1016/S0025-3227(00)00026-8.

Lebrun, J.-F., Lamarche, G., Collot, J.-Y., and Delteil, J., 2000, Abrupt strike-slip fault to subduction transition: The Alpine Fault–Puysegur Trench connection, New Zealand: Tectonics, v. 19, p. 688–706, https://doi.org/10.1029/2000TC900008.

Leeman, W.P., Tonarini, S., Chan, L.H., and Borg, L.E., 2004, Boron and lithium isotopic variations in a hot subduction zone—The southern Washington Cascades: Chemical Geology, v. 212, p. 101–124, https://doi.org/10.1016/j.chemgeo.2004.08.010.

Leeman, W.P., Tonarini, S., and Turner, S., 2017, Boron isotope variations in Tonga-Kermadec-New Zealand arc lavas: Implications for the origin of subduction components and mantle influences: Geochemistry Geophysics Geosystems, v. 18, p. 1126–1162, https://doi.org/10.1002/2016GC006523.

Lewis, K.B., and Marshall, B.A., 1996, Seep faunas and other indicators of methane-rich dewatering on New Zealand convergent margins: New Zealand Journal of Geology and Geophysics, v. 39, p. 181–200, https://doi.org/10.1080/00288306.1996.9514704.

Lewis, K.B., Collot, J.-Y., and Lallem, S.E., 1998, The dammed Hikurangi Trough: A channel-fed trench blocked by subducting seamounts and their wake avalanches (New Zealand–France GeodyNZ Project): Basin Research, v. 10, p. 441–468, https://doi.org/10.1046/j.1365-2117.1998.00080.x.

Li, L., Bonifacie, M., Aubaud, C., Crispi, O., Dessert, C., and Agrinier, P., 2015, Chlorine isotopes of thermal springs in arc volcanoes for tracing shallow magmatic activity: Earth and Planetary Science Letters, v. 413, p. 101–110, https://doi.org/10.1016/j.epsl.2014.12.044.

Millot, R., and Négrel, P., 2007, Multi-isotopic tracing (δ^7Li, δ^{11}B, ^{87}Sr/^{86}Sr) and chemical geothermometry: Evidence from hydro-geothermal systems in France: Chemical Geology, v. 244, p. 664–678, https://doi.org/10.1016/j.chemgeo.2007.07.015.

Millot, R., Scaillet, B., and Sanjuan, B., 2010, Lithium isotopes in island arc geothermal systems: Guadeloupe, Martinique (French West Indies) and experimental approach: Geochimica et Cosmochimica Acta, v. 74, p. 1852–1871, https://doi.org/10.1016/j.gca.2009.12.007.

Millot, R., Hegan, A., and Négrel, P., 2012, Geothermal waters from the Taupo Volcanic Zone, New Zealand: Li, B and Sr isotopes characterization: Applied Geochemistry, v. 27, p. 677–688, https://doi.org/10.1016/j.apgeochem.2011.12.015.

Moriguti, T., and Nakamura, E., 1998, Across-arc variation of Li isotopes in lavas and implication for crust/mantle recycling at subduction zones: Earth and Planetary Science Letters, v. 163, p. 167–174, https://doi.org/10.1016/S0012-821X(98)00184-8.

Mortimer, N., and Parkinson, D., 1996, Hikurangi Plateau: A Cretaceous large igneous province in the southwest Pacific Ocean: Journal of Geophysical Research, v. 101, p. 687–696, https://doi.org/10.1029/95JB03037.

Muramatsu, Y., Fehn, U., and Yoshida, S., 2001, Recycling of iodine in fore-arc areas: Evidence from the iodine brines in Chiba, Japan: Earth and Planetary Science Letters, v. 192, p. 583–593, https://doi.org/10.1016/S0012-821X(01)00483-6.

Musashi, M., Nomura, M., and Okamoto, M., 1988, Regional variation in the boron isotopic composition of hot spring waters from central Japan: Geochemical Journal, v. 22, p. 205–214, https://doi.org/10.2343/geochemj.22.205.

Palmer, M.R., and Sturchio, N.C., 1990, A boron isotope systematics of the Yellowstone National Park (Wyoming) hydrothermal system: A reconnaissance: Geochimica et Cosmochimica Acta, v. 54, p. 2811–2815, https://doi.org/10.1016/0016-7037(90)90015-D.

Palmer, M.R., and Swihart, G.H., 2002, Boron isotope geochemistry: An overview, *in* Grew, E.S., and Anovitz, L.M., eds., Boron: Mineralogy, Petrology, and Geochemistry (second printing with corrections and additions): Washington, D.C., Mineralogical Society of America, Reviews in Mineralogy, v. 33, p. 709–744.

Palmer, M.R., Spivack, A.J., and Edmond, J.M., 1987, Temperature and pH controls over isotopic fractionation during adsorption of boron on marine clay: Geochimica et Cosmochimica Acta, v. 51, p. 2319–2323, https://doi.org/10.1016/0016-7037(87)90285-7.

Peacock, S.M., and Hervig, R.L., 1999, Boron isotopic composition of subduction-zone metamorphic rocks: Chemical Geology, v. 160, p. 281–290, https://doi.org/10.1016/S0009-2541(99)00103-5.

Pecher, I.A., Henrys, S.A., Wood, W.T., Kukowski, N., Crutchley, G.J., Fohrmann, M., Kilner, J., Senger, K., Gorman, A.R., Coffin, R.B., Greinert, J., and Faure, K., 2010, Focussed fluid flow on the Hikurangi Margin, New Zealand—Evidence from possible local upwarping of the base of gas hydrate stability: Marine Geology, v. 272, p. 99–113, https://doi.org/10.1016/j.margeo.2009.10.006.

Penniston-Dorland, S.C., Sorensen, S.S., Ash, R.D., and Khadke, S.V., 2010, Lithium isotopes as a tracer of fluids in a subduction zone mélange: Franciscan Complex, CA: Earth and Planetary Science Letters, v. 292, p. 181–190, https://doi.org/10.1016/j.epsl.2010.01.034.

Penniston-Dorland, S.C., Bebout, G.E., Pogge von Strandmann, P.A., Elliott, T., and Sorensen, S.S., 2012, Lithium and its isotopes as tracers of subduction zone fluids and metasomatic processes: Evidence from the Catalina Schist, California, USA: Geochimica et Cosmochimica Acta, v. 77, p. 530–545, https://doi.org/10.1016/j.gca.2011.10.038.

Pettinga, J.R., 2003, Mud volcano eruption within the emergent accretionary Hikurangi margin, southern Hawke's Bay, New Zealand: New Zealand Journal of Geology and Geophysics, v. 46, p. 107–121, https://doi.org/10.1080/00288306.2003.9514999.

Pohatu, P., Warmenhoven, T., Rae, A., and Bradshaw, D., 2010, Low enthalpy geothermal energy resources for rural Māori communities—Te Puia Springs, East Coast, North Island New Zealand, *in* Proceedings, World Geothermal Congress, Bali, Indonesia, 25–29 April.

Qiu, L., Rudnick, R.L., Ague, J.J., and McDonough, W.F., 2011, A lithium isotopic study of sub-greenschist to greenschist facies metamorphism in an accretionary prism, New Zealand: Earth and Planetary Science Letters, v. 301, p. 213–221, https://doi.org/10.1016/j.epsl.2010.11.001.

Rait, G., Chanier, F., and Waters, D.W., 1991, Landward- and seaward-directed thrusting accompanying the onset of subduction beneath New Zealand: Geology, v. 19, p. 230–233, https://doi.org/10.1130/0091-7613(1991)019<0230:LASDTA>2.3.CO;2.

Ransom, B., Spivack, A.J., and Kastner, M., 1995, Stable Cl isotopes in subduction-zone pore waters: Implications for fluid-rock reactions and the cycling of chlorine: Geology, v. 23, p. 715–718, https://doi.org/10.1130/0091-7613(1995)023<0715:SCIISZ>2.3.CO;2.

Reyes, A.G., and Trompetter, W.J., 2012, Hydrothermal water–rock interaction and the redistribution of Li, B and Cl in the Taupo Volcanic Zone, New Zealand: Chemical Geology, v. 314–317, p. 96–112, https://doi.org/10.1016/j.chemgeo.2012.05.002.

Reyes, A.G., Christenson, B.W., and Faure, K., 2010, Sources of solutes and heat in low-enthalpy mineral waters and their relation to tectonic setting, New Zealand: Journal of Volcanology and Geothermal Research, v. 192, p. 117–141, https://doi.org/10.1016/j.jvolgeores.2010.02.015.

Richter, F.M., Mendybaev, R.A., Christensen, J.N., Hutcheon, I.D., Williams, R.W., Sturchio, N.C., and Beloso, J.A.D., 2006, Kinetic isotopic fractionation during diffusion of ionic species in water: Geochimica et Cosmochimica Acta, v. 70, p. 277–289, https://doi.org/10.1016/j.gca.2005.09.016.

Rudnick, R.L., and Gao, S., 2003, The composition of the continental crust, *in* Rudnick, R.L., ed., Treatise on Geochemistry, Volume 3: The Crust: New York, Elsevier, p. 1–64, https://doi.org/10.1016/B0-08-043751-6/03016-4.

Saffer, D.M., and Kopf, A.J., 2016, Boron desorption and fractionation in subduction zone fore arcs: Implications for the sources and transport of deep fluids: Geochemistry Geophysics Geosystems, v. 17, p. 4992–5008, https://doi.org/10.1002/2016GC006635.

Saffer, D.M., and Tobin, H.J., 2011, Hydrogeology and mechanics of subduction zone forearcs: Fluid flow and pore pressure: Annual Review of Earth and Planetary Sciences, v. 39, p. 157–186, https://doi.org/10.1146/annurev-earth-040610-133408.

Savov, I.P., Ryan, J.G., D'Antonio, M., Kelley, K., and Mattie, P., 2005, Geochemistry of serpentinized peridotites from the Mariana Forearc Conical Seamount, ODP Leg 125: Implications for the elemental recycling at subduction zones: Geochemistry Geophysics Geosystems, v. 6, Q04J15, https://doi.org/10.1029/2004GC000777.

Selverstone, J., and Sharp, Z.D., 2015, Chlorine isotope behavior during prograde metamorphism of sedimentary rocks: Earth and Planetary Science Letters, v. 417, p. 120–131, https://doi.org/10.1016/j.epsl.2015.02.030.

Seyfried, W.E., Janecky, D.R., and Mottl, M.J., 1984, Alteration of the oceanic crust: Implications for geochemical cycles of lithium and boron: Geochimica et Cosmochimica Acta, v. 48, p. 557–569, https://doi.org/10.1016/0016-7037(84)90284-9.

Seyfried, W.E., Chen, X., and Chan, L.-H., 1998, Trace element mobility and lithium isotope exchange during hydrothermal alteration of seafloor weathered basalt: An experimental study at 350°C, 500 bars: Geochimica et Cosmochimica Acta, v. 62, p. 949–960, https://doi.org/10.1016/S0016-7037(98)00045-3.

Shinohara, H., 2013, Volatile flux from subduction zone volcanoes: Insights from a detailed evaluation of the fluxes from volcanoes in Japan: Journal of Volcanology and Geothermal Research, v. 268, p. 46–63, https://doi.org/10.1016/j.jvolgeores.2013.10.007.

Sibson, R.H., and Rowland, J.V., 2003, Stress, fluid pressure and structural permeability in seismogenic crust, North Island, New Zealand: Geophysical Journal International, v. 154, p. 584–594, https://doi.org/10.1046/j.1365-246X.2003.01965.x.

Spivack, A.J., Kastner, M., and Ransom, B., 2002, Elemental and isotopic chloride geochemistry and fluid flow in the Nankai Trough: Geophysical Research Letters, v. 29, no. 14, https://doi.org/10.1029/2001GL014122.

Stefánsson, A., and Barnes, J.D., 2016, Chlorine isotope geochemistry of Icelandic thermal fluids: Implications for geothermal system behavior at divergent plate boundaries: Earth and Planetary Science Letters, v. 449, p. 69–78, https://doi.org/10.1016/j.epsl.2016.05.041.

Straub, S.M., and Layne, G.D., 2002, The systematics of boron isotopes in Izu arc front volcanic rocks: Earth and Planetary Science Letters, v. 198, p. 25–39, https://doi.org/10.1016/S0012-821X(02)00517-4.

Taran, Y.A., 2009, Geochemistry of volcanic and hydrothermal fluids and volatile budget of the Kamchatka–Kuril subduction zone: Geochimica et Cosmochimica Acta, v. 73, p. 1067–1094, https://doi.org/10.1016/j.gca.2008.11.020.

Teng, F.-Z., McDonough, W.F., Rudnick, R.L., Dalpé, C., Tomascak, P.B., Chappell, B.W., and Gao, S., 2004, Lithium isotopic composition and concentration of the upper continental crust: Geochimica et Cosmochimica Acta, v. 68, p. 4167–4178, https://doi.org/10.1016/j.gca.2004.03.031.

Teng, F.-Z., McDonough, W.F., Rudnick, R.L., Walker, R.J., and Sirbescu, M.-L.C., 2006, Lithium isotopic systematics of granites and pegmatites from the Black Hills, South Dakota: American Mineralogist, v. 91, p. 1488–1498, https://doi.org/10.2138/am.2006.2083.

Tomascak, P.B., Magna, T., and Dohmen, R., 2016, Advances in Lithium Isotope Geochemistry: Berlin, Springer, 195 p., https://doi.org/10.1007/978-3-319-01430-2.

Tonarini, S., Pennisi, M., and Leeman, W.P., 1997, Precise boron analysis of complex silicate (rock) samples using alkali carbonate fusion and ion exchange separation: Chemical Geology, v. 142, p. 129–137, https://doi.org/10.1016/S0009-2541(97)00087-9.

Townend, J., 1997, Subducting a sponge: Minimum estimates of the fluid budget of the Hikurangi margin accretionary prism: Geological Society of New Zealand Newsletter, no. 112, p. 14–16.

Verney-Carron, A., Vigier, N., and Millot, R., 2011, Experimental determination of the role of diffusion on Li isotope fractionation during basaltic glass weathering: Geochimica Et Cosmochimica Acta, v. 75, p. 3452–3468, https://doi.org/10.1016/j.gca.2011.03.019.

Völker, D., Wehrmann, H., Kutterolf, S., Iyer, K., Rabbel, W., Geersen, J., and Hoernle, K., 2014, Constraining input and output fluxes of the southern-central Chile subduction zone: Water, chlorine and sulfur: International Journal of Earth Sciences, v. 103, p. 2129–2153, https://doi.org/10.1007/s00531-014-1002-0.

Wallace, L.M., and Beavan, J., 2010, Diverse slow slip behavior at the Hikurangi subduction margin, New Zealand: Journal of Geophysical Research, v. 115, B12402, https://doi.org/10.1029/2010JB007717.

Wallace, L.M., Beavan, J., McCaffrey, R., and Darby, D., 2004, Subduction zone coupling and tectonic block rotations in the North Island, New Zealand: Journal of Geophysical Research, v. 109, B12406, https://doi.org/10.1029/2004JB003241.

Wallace, L.M., Reyners, M., Cochran, U., Bannister, S., Barnes, P.M., Berryman, K., Downes, G., Eberhart-Phillips, D., Fagereng, A., Ellis, S., Nicol, A., McCaffrey, R., Beavan, R.J., Henrys, S., Sutherland, R., Barker, D.H.N., Litchfield, N., Townend, J., Robinson, R., Bell, R., Wilson, K., and Power, W., 2009, Characterizing the seismogenic zone of a major plate boundary subduction thrust: Hikurangi Margin, New Zealand: Geochemistry, Geophysics, Geosystems, v. 10, Q10006, https://doi.org/10.1029/2009GC002610.

Wallace, L.M., Bell, R., Townend, J., Ellis, S., Bannister, S., Henrys, S., Sutherland, R., and Barnes, P., 2010, Subduction systems revealed: Studies of the Hikurangi margin: Eos (Transactions, American Geophysical Union), v. 45, p. 417–418, https://doi.org/10.1029/2010EO450001.

Wallace, L.M., Fagereng, Å., and Ellis, S., 2012, Upper plate tectonic stress state may influence interseismic coupling on subduction megathrusts: Geology, v. 40, p. 895–898, https://doi.org/10.1130/G33373.1.

Wallace, P.J., 2005, Volatiles in subduction zone magmas: Concentrations and fluxes based on melt inclusion and volcanic gas data: Journal of Volcanology and Geothermal Research, v. 140, p. 217–240, https://doi.org/10.1016/j.jvolgeores.2004.07.023.

Wei, W., Kastner, M., Deyhle, A., and Spivack, A.J., 2005, Geochemical cycling of fluorine, chlorine, bromine, and boron and implications for fluid-rock reactions in Mariana forearc, South Chamorro Seamount, ODP Leg 195, *in* Shinohara, M., Salisbury, M.H., and Richter, C., eds., Proceedings of the Ocean Drilling Program, Scientific Results, Volume 195: College Station, Texas, Ocean Drilling Program, 23 p., https://doi.org/10.2973/odp.proc.sr.195.106.2005.

Wilson, C.J.N., Houghton, B.F., McWilliams, M.O., Lanphere, M.A., Weaver, S.D., and Briggs, R.M., 1995, Volcanic and structural evolution of Taupo Volcanic Zone, New Zealand: A review: Journal of Volcanology and Geothermal Research, v. 68, p. 1–28, https://doi.org/10.1016/0377-0273(95)00006-G.

Wood, R., and Davy, B., 1994, The Hikurangi Plateau: Marine Geology, v. 118, p. 153–173, https://doi.org/10.1016/0025-3227(94)90118-X.

Wunder, B., Meixner, A., Romer, R.L., Wirth, R., and Heinrich, W., 2005, The geochemical cycle of boron: Constraints from boron isotope partitioning experiments between mica and fluid: Lithos, v. 84, p. 206–216, https://doi.org/10.1016/j.lithos.2005.02.003.

You, C.-F., Spivack, A.J., Smith, J.H., and Gieskes, J.M., 1993, Mobilization of boron in convergent margins: Implications for the boron geochemical cycle: Geology, v. 21, p. 207–210, https://doi.org/10.1130/0091-7613(1993)021<0207:MOBICM>2.3.CO;2.

You, C.-F., Spivack, A.J., Gieskes, J.M., Martin, J.B., and Davisson, M.L., 1996, Boron contents and isotopic composition in pore waters: A new approach to determine temperature induced artifacts—Geochemical applications: Marine Geology, v. 129, p. 351–361, https://doi.org/10.1016/0025-3227(96)83353-6.

Zack, T., Tomascak, P.B., Rudnick, R.L., Dalpé, C., and McDonough, W.F., 2003, Extremely light Li in orogenic eclogites: The role of isotope fractionation during dehydration in subducted oceanic crust: Earth and Planetary Science Letters, v. 208, p. 279–290, https://doi.org/10.1016/S0012-821X(03)00035-9.

Zhang, M., Hobbs, M.Y., Frape, S.K., Nordstrom, D.K., Ball, J.W., and McCleskey, R.B., 2004, Stable chlorine isotopic composition of geothermal waters from Yellowstone National Park, *in* Wanty, R.B., and Seal, R.R., eds., Water-Rock Interactions: Proceedings of the Eleventh International Symposium on Water-Rock Interaction, Volume 1: London, Taylor and Francis Group, p. 233–236.